The Fueling and Evolution of AGN: Internal and External Triggers

Shardha Jogee[1]

Space Telescope Science Institute, 3700 San Martin Drive, Baltimore MD 21218, U.S.A jogee@stsci.edu

1 Introduction

The quest for a coherent picture of nuclear activity has witnessed giant leaps in the last decades. Four decades ago, the idea was put forward that accretion of matter onto a massive compact object or a supermassive black hole (SMBH) of mass $> 10^6$ $M_\odot$ could power very luminous active galactic nuclei (AGN), in particular, quasi-stellar objects (QSOs) (Lynden-Bell 1969; Soltan 1982; Rees 1984). In the last decade, dynamical evidence increasingly suggests that SMBH pervade the centers of most massive galaxies (§ 2 and references therein). The challenge has now shifted towards probing the fueling and evolution of AGN over a wide range of cosmic lookback times, and elucidating how they relate to their host galaxies in both the local and cosmological context.

In this review, I will focus on the fueling and evolution of AGN under the influence of internal and external triggers. In the nature versus nurture paradigm, I use the term internal triggers to refer to intrinsic properties of host galaxies (e.g., morphological or Hubble type, color, and non-axisymmetric features such as large-scale bars and nuclear bars) while external triggers refer to factors such as environment and interactions. The distinction is an over-simplification as many of the so called intrinsic properties of galaxies can be induced or dissolved under the influence of external triggers. Connections will be explored between the nuclear and larger-scale properties of AGN, both locally and at intermediate redshifts. One of the driving objectives is to understand why not all relatively massive galaxies show signs of AGN activity (via high-excitation optical lines or X-ray emission) despite mounting dynamical evidence that they harbor SMBHs. The most daunting challenge in fueling AGN is arguably the angular momentum problem (§ 3.2). Even matter located at a radius of a few hundred pc must lose more than 99.99% of its specific angular momentum before it is fit for consumption by a BH.

The sequence of this review is as follows. § 2 briefly addresses BH demographics and the BH-bulge-halo correlations. § 3 sets the stage for the rest of this paper by providing an overview of central issues in the fueling of AGN and circumnuclear starbursts. In particular, I review mass accretion rates, angular momentum requirements, the effectiveness of different fueling

mechanisms, and the growth and mass density of BHs at different epochs. These central issues in § 3 are attacked in more detail in § 4–9 which describe different fueling mechanisms including mergers and interactions (§ 5), large-scale bars (§ 6), nuclear bars (§ 7), nuclear spirals (§ 8), and processes relevant on hundred pc to sub-pc scales (§ 9). I conclude with a summary and future perspectives in § 10. Complementary reviews on mass transfer and central activity in galaxies include those by Shlosman (2003), Combes (2003), Knapen (2004), and Martini (2004).

2 BH Demographics and BH-Bulge-Halo Correlations

2.1 Measurement of BH Masses

The term SMBHs refers to BHs having masses $M_{\rm bh} > 10^6$ M$_\odot$, in contrast to intermediate mass BHs (IMBHs) with $M_{\rm bh} \sim 10^2$–10^6 M$_\odot$, and stellar mass BHs. Properties of SMBHs are generally studied through accretion signatures of BHs or their gravitational influence. The strongest dynamical evidence for SMBHs are in our Galaxy and in NGC 4258. In these systems, the large central densities inferred within a small resolved radius can be accounted for by a SMBH, but not by other possibilities such as collections of compact objects, star clusters, or exotic particles. In our Galaxy, proper motion measurements set stringent constraints on the central potential (Schödel et al. 2003; Ghez et al. 2003; Genzel et al. 2000), yielding $M_{\rm bh} \sim 3$–4×10^6 M$_\odot$. In NGC 5248, VLBA maser observations reveal Keplerian motions implying $M_{\rm bh} \sim 3.9 \times 10^7$ M$_\odot$ (Miyoshi et al. 95).

In the last decade, high resolution gas and stellar dynamical measurements from ground-based (e.g., Kormendy & Richstone 1995) and *HST* observations (e.g., Harms et al. 1994; Ferrarese et al. 1996 ; van de Marel & van den Bosch 1998; Ferrarese & Ford 99; Gebhardt et al. 2000) have provided compelling evidence that several tens of galaxies host massive central dark objects (CDOs) which are likely to be SMBHs. The more reliable dynamical measurements tend to be from observations which resolve the radius of influence ($R_{\rm g-bh}$) within which the gravitational force of the BH exceeds that of nearby stars with velocity dispersion σ, namely,

$$R_{\rm g-bh} = \frac{GM_{\rm bh}}{\sigma^2} = 11.2 \text{ pc} \left(\frac{M_{\rm bh}}{10^8 \text{ M}_\odot}\right) \left(\frac{\sigma}{200 \text{ km s}^{-1}}\right)^{-2} \quad (1)$$

However, the scales probed by these measurements are still several 10^5–10^6 times the Schwarzschild radius ($R_{\rm s-bh}$) of the BH, namely,

$$R_{\rm s-bh} = \frac{2GM_{\rm bh}}{c^2} = 5 \times 10^{-4} \text{ pc} \left(\frac{M_{\rm bh}}{10^8 \text{ M}_\odot}\right) \quad (2)$$

The majority of the afore mentioned reliable measurements target ellipticals and a few early-type (Sa-Sbc) spirals with central $\sigma < 60$ km s^{-1}, and

probe BH masses in the range 10^7–10^9 $M_\odot$. Conversely, measuring BH masses in late-type spirals and dwarf galaxies poses many challenges, and there are no firm measurements of BH masses below 10^6 $M_\odot$. However, theoretical models and a mounting body of observational evidence put the existence of IMBHs on a relatively firm footing (see review by van der Marel 2003). The first challenge in measuring the masses of IMBHs is that the gravitational radii of such BHs are typically too small to be easily resolved even with *HST*. A second complication is that late-type spirals and dwarf galaxies which might harbor such BHs also tend to host a bright 10^6–10^7 $M_\odot$ stellar cluster (Boker et al. 1999) whose dynamical effect can mask that of the BH. A 10^4–10^5 $M_\odot$ BH (Filipenko & Ho 2003) has been invoked in the Sm dwarf NGC 4395 which hosts the nearest and lowest luminosity Seyfert 1 nucleus. Upper limits on BH masses are reported in several systems, e.g., 10^6–10^7 $M_\odot$ for six dwarf ellipticals in Virgo (Geha, Guhathakurta, & van der Marel 2002), 5×10^5 $M_\odot$ for the Scd spiral IC342 (Boker et al.1999). Gebhardt, Rich, & Ho (2002) infer the presence of an IMBH with a mass of a few $\times$ 10^4 $M_\odot$ in one of the most massive stellar clusters (G1) in M31, but an alternative interpretation of the dataset has been presented by Baumgardt et al. (2003). A tantalizing dark central mass concentration of a few $\times 10^3$ $M_\odot$ (Gerssen et al. 2003) is reported in the globular cluster M15 from *HST* data, but it remains unclear whether it is an IMBH. *Chandra* observations of ultraluminous X-ray sources also suggest the presence of IMBHs (Clobert & Miller 2004 and references therein).

At many levels, measuring BH masses in local AGN such as Seyferts and LINERS is more challenging than corresponding measurements in massive quiescent galaxies. The bright non-thermal active nucleus in Seyfert galaxies can drown the spectroscopic features from which dynamical measurements are made. Consequently, BH masses in local AGN are commonly mapped with alternative techniques such as reverberation mapping (Blandford & Mc Kee 1982; Peterson 1993; see Peterson these proceedings) where one estimates the virial mass inside the broad-line region (BLR) by combining the velocity of the BLR with an estimate of the size of the BLR based on time delay measurements. Reverberation mapping can typically probe scales $\sim$ 600 $R_{\rm s-bh}$ and has yielded BH masses for several tens of AGN (Peterson 1993; Wandel, Peterson, & Malkan 1999; Kaspi 2000). Earlier controversies existed on the reliability of the method due to purported systematic differences in the BH-to-bulge mass ratio between AGN with reverberation mapping data and quiescent galaxies or QSOs. However, recent work (e.g., Ferrarese et al. 2001) claims that for AGN with accurate measurements of stellar velocity dispersions, the reverberation masses agree with the BH mass determined from the tight $M_{\rm bh}$–σ relation (§ 2.2) which is derived from quiescent galaxies.

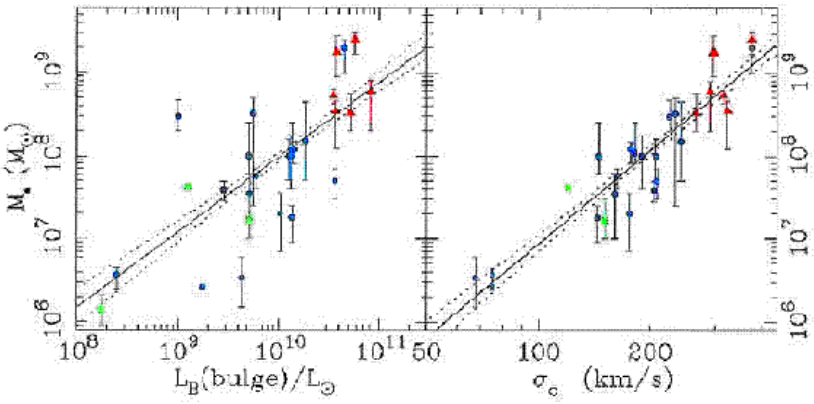

Fig. 1. Correlation between central BH mass and circumnuclear velocity dispersion – Black hole mass versus bulge luminosity (left) and the luminosity-weighted aperture dispersion within the effective radius (right). Green squares denote galaxies with maser detections, red triangles are from gas kinematics, and blue circles are from stellar kinematics. Solid and dotted lines are the best-fit correlations and their 68 % confidence bands. (From Gebhardt et al. 2000)

2.2 Relationship of the Central BH to the Bulge and Dark Halo

A tight correlation has been reported between the mass of a central BH and the stellar velocity dispersion (σ) of the host galaxy's bulge (Ferrarese & Merritt 2000; Gebhardt et al. 2000):

$$M_{\rm h} = \alpha \left(\frac{\sigma}{200 \text{ km s}^{-1}} \right)^{\beta} \text{ M}_{\odot} \tag{3}$$

where $\alpha = (1.7 \pm 0.3) \times 10^8$, $\beta = (4.8 \pm 0.5)$ (Ferrarese & Merritt 2000), and $\alpha = (1.2 \pm 0.2) \times 10^8$, $\beta = (3.8 \pm 0.3)$ (Gebhardt et al. 2000). Tremaine et al. (2002) assign the range in quoted values for β to systematic differences in velocity dispersions used by different groups. The $M_{\rm bh}$–σ relation reported originally in the literature (Gebhardt et al. 2000; Ferrarese & Merritt 2000; Tremaine et al. 2002) is primarily based on local early-type galaxies (E/SOs) and a handful of spirals Sb–Sbc, and it primarily samples quiescent BHs with masses in the range a few $\times$ (10^7–10^9) $\text{M}_{\odot}$. This relation was subsequently found to also hold in AGN hosts (Ferrarese et al. 2001), and in bright QSOs out to $z \sim 3$ with estimated BH masses of up to 10^{10} $\text{M}_{\odot}$ (Shields et al. 2003). *This suggests that active and quiescent BHs bear a common relationship to the surrounding triaxial component of their host galaxies over a wide range of cosmic epochs and BH masses* (10^6–10^{10} $\text{M}_{\odot}$).

Numerous variants of the $M_{\rm bh}$–σ relation have been proposed. While earlier correlations between the mass of CDOs/SMBHs and the bulge luminosity ($L_{\rm bulge}$) had significant scatter (e.g., Kormendy & Richstone 1995), recent

work (Häring & Rix 2004) based on improved BH and bulge masses yield a very tight $M_{\rm bh}$–$M_{\rm bulge}$ relation. Graham et al. (2001) find a correlation between the light concentration of galaxies and the mass of their SMBHs, and claim this relation is as tight as the $M_{\rm bh}$–σ relation. Grogin et al. (2004) have searched for signs of this correlation at $z \sim 0.4$–1.3 in a comparative study of structural parameters among 34000 galaxies in the GOODS fields, including 350 X-ray selected AGN hosts in the overlapping *Chandra* Deep Fields. Compared to the inactive galaxies, the AGN hosts have significantly enhanced concentration indices throughout the entire redshift range, as measured in rest frame B-band for a volume-limited sample to $M_{\rm B} <$ -19.5 (and to L(2–8keV) $> 10^{42}$ for the AGN). Finally, Ferrarese (2002) shows that the $M_{\rm bh}$–σ relation translates to a relation between the mass of the BH and that of the dark matter (DM) halo ($M_{\rm dm}$)

$$M_{\rm h} \ = 10^7 \ {\rm M}_\odot \left(\frac{M_{\rm dm}}{10^{12} \ {\rm M}_\odot} \right)^{1.65} \tag{4}$$

if one assumes that σ correlates with the circular speed $V_{\rm c}$ which bears an intimate relation to the DM halo within the standard ΛCDM paradigm.

A plethora of theoretical studies have explored the growth of BHs and the possible origin of a fundamental $M_{\rm bh}$–σ relation (e.g., Haehnelt & Kauffmann 2000; Adams, Graff, & Richstone 2001; Burkert & Silk 2001; Di Matteo, Croft, Springel, & Hernquist 2003; Bromm & Loeb 2003; Wyithe & Loeb 2003; El-Zant et al. 2003). According to Haehnelt & Kauffmann (2000), hierarchical galaxy formation models where bulges and SMBHs both form during major mergers produce a $M_{\rm bh}$–σ correlation. Star-formation (SF) regulated growth of BHs in protogalactic spheroids has been proposed by Burkert & Silk (2001) and Di Matteo et al. (2003). In many of these models, black hole growth stops because of the competition with SF and, in particular, feedback, both of which determine the gas fraction available for accretion. According to Wyithe & Loeb (2003), a tight $M_{\rm bh}$–σ relation naturally results from hierarchical ΛCDM merging models where SMBHs in galaxy centers undergo self-regulated growth within galaxy halos until they unbind the galactic gas that feeds them. El-Zant et al. (2003) have suggested that the BH–bulge–DM halo correlation can be understood within the framework of galactic structures growing within flat-core, mildly triaxial halos.

3 Central Issues in Fueling AGN and Starbursts

I present here an overview of several central issues that are relevant for understanding the fueling of AGN and circumnuclear starbursts.

3.1 Mass Accretion Rates

For a standard BH accretion disk with an efficiency ϵ of conversion between matter and energy, the radiated bolometric luminosity $L_{\rm bol}$ is related to the mass accretion rate ($\dot{M}_{\rm bh}$) at the last stable orbit of a BH by

$$\dot{M}_{\rm bh} = 0.15\ {\rm M}_\odot\ {\rm yr}^{-1}\ \left(\frac{0.1}{\epsilon}\right)\ \left(\frac{L_{\rm bol}}{10^{45}\ {\rm ergs\ s}^{-1}}\right) \quad (5)$$

Table 1 shows typical observed bolometric luminosities and inferred mass accretion rates for QSOs and local AGN (Seyfert, LINERS) assuming a standard radiative efficiency $\epsilon \sim 0.1$. The standard value of $\epsilon \sim 0.1$ applies if the gravitational binding energy liberated by the accreting gas at the last stable orbit of the BH is radiated with an efficiency of $\sim 0.1\ c^2$. In practice, the radiative efficiency depends on the nature of the accretion disk and gas accretion flows. For instance, thin-disk accretion onto a Kerr BH can lead to a radiative efficiency $\epsilon \sim 0.2$. It has been suggested that the most luminous quasars at high redshift may have grown with $\epsilon \sim 0.2$, or alternatively that they have a super-Eddington luminosity (Yu & Tremaine 2002). Conversely, in certain popular models of gas accretion flows such as adiabatic inflow-outflow solutions (ADIOS; Blandford & Begelman 1999) and convection-dominated accretion flows (CDAF: Narayan et al. 2000) only a small fraction of the matter which accretes at the outer boundary of the flow contributes to the mass accretion rate at the BH due to turbulence and strong mass loss. This leads to an effective radiation efficiency $\ll 0.1$ when applied to the mass accretion rate at the outer boundary of the accretion flow. Thus, within the CDAF and ADIOS paradigms, the gas inflow rates that must be supplied on scales of tens of pc may be much larger than those quoted in Table 1, even for low luminosity Seyferts.

Table 1. Typical $L_{\rm bol}$ and $\dot{M}_{\rm bh}$ for QSOs and local AGN

Type of AGN	$L_{\rm bol}$[a] (ergs s^{-1})	Typical $L_{\rm bol}$ (ergs s^{-1})	Typical $\dot{M}_{\rm bh}$[b] (M$_\odot$ yr^{-1})
(1)	(2)	(3)	(4)
QSOs	10^{46}–10^{48}	10^{47}–10^{48}	10–100
Seyferts	10^{40}–10^{45}	10^{43}-10^{44}	10^{-3}–10^{-2}
LINERs	10^{39}–$10^{43.5}$	10^{41}–10^{42}	10^{-5}–10^{-4}

Notes to Table – a. The full range in bolometric luminosity ($L_{\rm bol}$) for Seyfert and LINERS is taken from Ho, Filippenko, & Sargent 1997a, while for QSOs different sources in the literature are used; b. The typical $\dot{M}_{\rm bh}$ in column (4) is derived from the typical $L_{\rm bol}$ in column (3) assuming a standard radiative efficiency $\epsilon \sim 0.1$

3.2 The Angular Momentum Problem

The most important challenge in fueling AGN is the angular momentum problem rather than the amount of fuel *per se.* The angular momentum per unit mass or specific angular momentum $L{=}r \times v$ of fuel at the last stable radius of a BH of mass ($M_8 \times 10^8$ $M_\odot$) is several times $10^{24} M_8$ cm^2 s^{-1}. In contrast, matter (star or gas) rotating in a spiral or elliptical galaxy at a radius of 10 kpc has a specific angular momentum of several times $10^{29} M_8$ cm^2 s^{-1}. This is illustrated in Fig. 2 assuming typical galactic rotation velocities. Thus, *the specific angular momentum of matter located at a radius of a few kpc must be reduced by more than 10^4 before it is fit for consumption by a BH.* Searching for mechanisms which can achieve this miraculous reduction of angular momentum is one of the driving objectives of AGN research. Even at a radius of 200 pc, L is still a factor of 1000 too large, and the angular momentum barrier is a more daunting challenge than the amount of gas. For instance, in the case of a Seyfert with an accretion rate of $\sim 10^{-2}$ $M_\odot$ yr^{-1} and a duty cycle of 10^8 years, a gas cloud of 10^6 $M_\odot$ may provide adequate fuel. Such clouds are certainly common within the inner 200 pc radius of spiral galaxies, but we yet have to understand what physical processes are able to squeeze their angular momentum out by more than 99.99%. The BH is analogous to an exigent dieter who has a plentiful supply of rich food, but can only consume 99.9% fat-free items!

3.3 Dominant Fueling Mechanisms on Different Scales

Gravitational torques, dynamical friction, viscous torques, and hydrodynamical torques (shocks) are some of the mechanisms which remove angular momentum from the dissipative gas component and channel it to small scales, thereby helping to fuel central starbursts and massive BHs. These different fueling mechanisms assume a different relative importance at different radii in a galaxy, and also, when dealing with a strongly interacting galaxy versus an isolated one. I will review these different mechanisms in detail from an observational and theoretical perspective in § 4–9, but here I discuss a few key concepts and provide a schematic overview in Fig. 2.

Table 2. Gravitational Torques, Dynamical Friction, and Viscous Torques

R (pc) (1)	M ($M_\odot$) (2)	$t_{\rm gra}$ (Myr) (3)	$t_{\rm df}$ (Myr) (4)	$t_{\rm visc}$ (Myr) (5)
1000	1e7	20	1020	1000
200	1e7	4	60	-

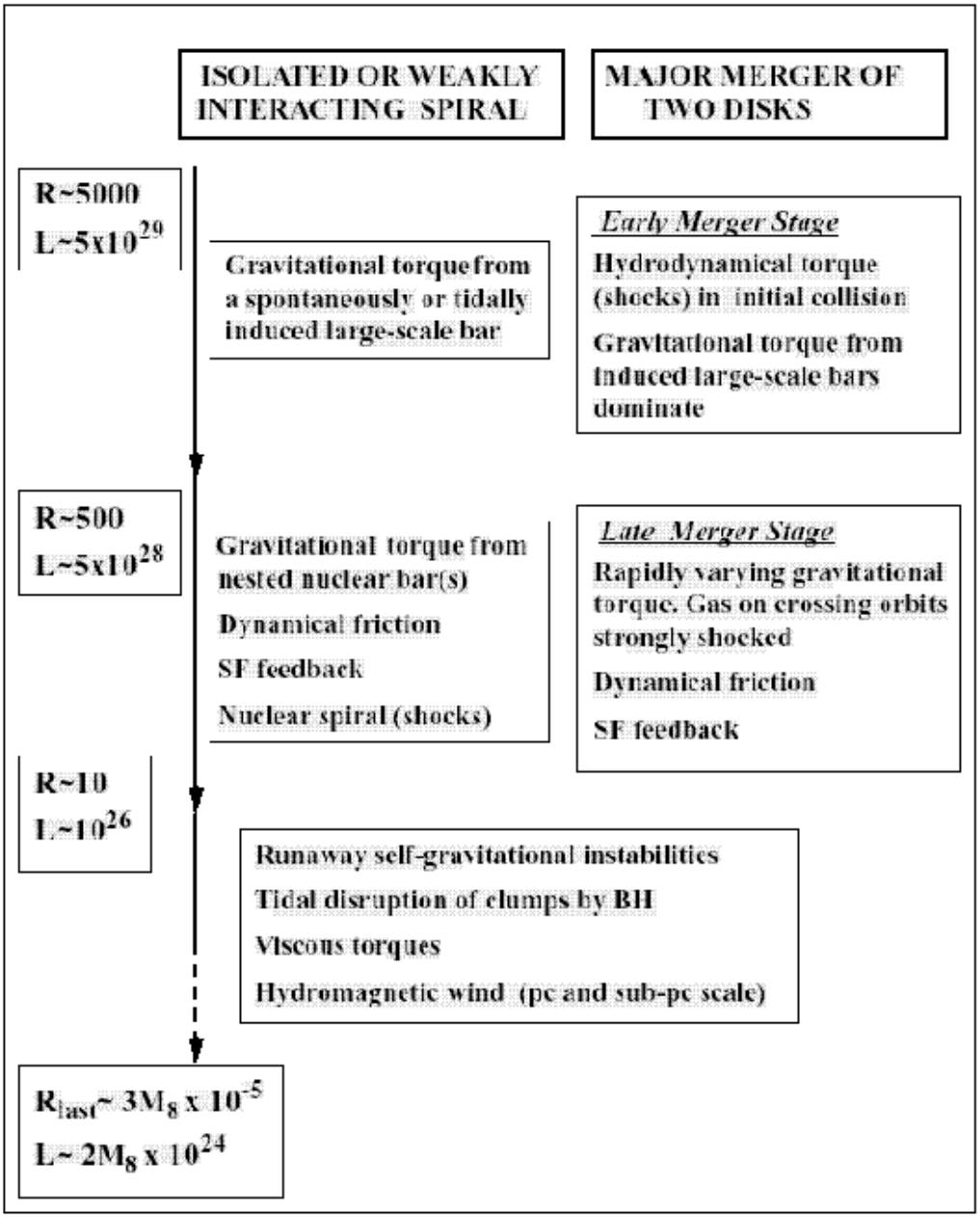

Fig. 2. The angular momentum problem in the fueling of AGN and starbursts: The specific angular momentum (L) of gas located at a radius (R) of several kpc must be reduced by more than 10^4 before it is fit for consumption at the last stable orbit ($R_{\rm last}$) of a BH. In contrast, powerful starbursts can be more easily triggered via gravitational torques which build large gas densities on circumnuclear (R=500 pc) scales. This figure schematically illustrates some mechanisms that can reduce L and drive gas inflow on various spatial scales in a relatively quiescent galaxy *(left)* and in a major merger *(right)*. R is in pc, L is in units of cm^2 s^{-1}, and a ($M_8 \times 10^8$ M$_\odot$) BH is assumed. See text for details.

Gravitational torques operate on a timescale ($t_{\rm gra}$) comparable to the orbital timescale and provide, therefore, the most efficient way of reducing angular momentum on large to intermediate scales (tens of kpc – a few 100 pc). This can be seen by comparing $t_{\rm gra}$ with the typical timescales on which dynamical friction ($t_{\rm df}$) and viscous torques ($t_{\rm vis}$) operate for a cloud of mass M (Table 2). Dynamical friction on a clump of mass M and speed v at a radius R operates on a timescale which is $\propto (R^2\ v/M\ \ln\Lambda)$, where $\ln\Lambda$ is the Coulomb logarithm (Binney & Tremaine 1987). For a 10^7 $M_\odot$ gas cloud at a kpc radius in a disk galaxy, $t_{\rm df}$ is an order of magnitude larger than $t_{\rm gra}$ (Table 2). However, for massive gas clumps at low radii, dynamical friction becomes increasingly important: it can drive a 10^8 $M_\odot$ cloud from $R \sim 200$ pc down to $R \sim 10$ pc within a few times 10^7 yrs (§ 9).

In an isolated galaxy (Fig. 2), gravitational torques are exerted by non-axisymmetric features such as large-scale (§ 6) and nuclear (§ 7) bars. While a large-scale bar efficiently drives gas from the outer disk into the inner kpc, the bar-driven gas flow slows or even stalls as it crosses the inner Lindblad resonance (ILR) for reasons described in § 6. At this stage, the gas piles up typically at a radius of several 100 pc where powerful starbursts are commonly observed (§ 6; Fig 6). However, gas on these scales has a specific angular momentum that is still more than 1000 times too high for it to be digestible by a BH. If a nuclear bar (§ 7) is present, it can break the status quo and torque gas from the ILR region of the large-scale bar down to tens of pc. In addition, if massive gas clumps exist in the inner few 100 pc, dynamical friction can drive them down to tens of pc (§ 9). Finally, feedback from SF (e.g., shocks from supernovae) can remove energy and angular momentum (§ 9) from a small fraction of the circumnuclear gas. On scales of tens of pc, the tidal torque from the BH itself can disrupt gas clumps and stellar clusters, possibly into an accretion disk (§ 9). Subsequently, on pc and sub-pc scales, viscous torques and hydromagnetic outflows in AGN (§ 9) may become important.

Simulations suggest that induced large-scale stellar bars remain the main driver of gas inflows down to scales of a few 100 pc, even in the case of interacting galaxies (Fig. 2), namely in many minor mergers (§ 5.2) and during the *early* stages of major (1:1) and intermediate mass ratio (1:3) interactions (§ 5.1). Just like in the case of an isolated barred galaxy, gas inflows driven by an induced bar also slow down near the ILR. However, the *final stages* of a major or intermediate mass ratio merger bring in very different elements. As violent relaxation starts, gas experiences strongly-varying gravitational torques, and if it is on interacting and crossing orbits, it also suffers strong shocks (§ 5.1; Fig. 2). Thus, in the final merger stages, gas loses angular momentum and large gas inflows ($\gg 1 M_\odot$ yr^{-1}) down to small scales can result, provided the earlier episodes of SF have not depleted most of the circumnuclear gas already (§ 5.1).

3.4 Census and Growth Epoch of BHs

Table 3 compares the BH mass density ($\rho_{\rm bh-qso}$) accreted during the optically bright QSO phases (z=0.2–5) to the BH mass density in present-day galaxies (both active and inactive). Yu & Tremaine (2002) find $\rho_{\rm bh-qso} \sim (2.5 \pm 0.4) \times 10^5\ (h_0/65)^2\ {\rm M}_\odot\ {\rm Mpc}^{-3}$ using the extrapolated QSO luminosity function from the 2dF redshift survey and a radiative efficiency of 0.1. Similar values have been reported by others including Wyithe & Loeb (2003), Ferrarese (2002b), and Chokshi & Turner (1992). This value of $\rho_{\rm bh-qso}$ is a lower limit to the total BH mass density we expect to be in place by z=0.2 since it does not incorporate optically obscured QSOs and any build-up of the BH mass occurring outside the QSO phase. However, it is probably not far off, since the BH mass density from X-ray AGN counts at $z > 0.2$ ($\rho_{\rm bh-xray}$) is estimated to be 2–5 $\times\ 10^5\ {\rm M}_\odot\ {\rm Mpc}^{-3}$ (Cowie & Barger 2004; Fabian & Iwasawa 1999; Table 3).

Table 3. Census of BH Mass density

BH Mass Density [$10^5\ {\rm M}_\odot\ {\rm Mpc}^{-3}$]	
$\rho_{\rm bh-QSO}$ accreted during optical QSO phase (z=0.2–5)	2–4[a,b,c,d]
$\rho_{\rm bh-Xray}$ from X-ray background ($z > 0.2$)	2–5[e,f]
$\rho_{\rm bh-local}$ in local early-type galaxies ($z < 0.1$)	2–6[a,b,g]
$\rho_{\rm bh-Sy}$ in local Seyferts	< 0.5[c]

References in table – a. Yu & Tremaine 2002; b. Wyithe & Loeb 2003; c. Ferrarese 2002; d. Chokshi & Turner 1992; e. Cowie & Barger 2004; f. Fabian & Iwasawa 1999; g. Merritt & Ferrarese 2001.

In the local Universe, the BH mass density in early-type galaxies at $z < 0.1$ is estimated to be $(2.5 \pm 0.4) \times 10^5\ (h_0/65)^2\ {\rm M}_\odot\ {\rm Mpc}^{-3}$, based on the measured velocity dispersion of early-type galaxies in the Sloan Digital Sky Survey and the $M_{\rm bh}$–σ relation (Yu & Tremaine 2002). However, rough estimates of the BH mass density in local *active* Seyfert 1 and 2 galaxies yield significantly lower values (Ferrarese 2002; Padovani et al. 1990; Table 3).

In summary, the census of BH mass density (Table 3) suggests that accretion with a standard radiation efficiency of 0.1 during the quasar era can readily account for the BH mass density found in local ($z < 0.1$) early-type galaxies. Only a small fraction of this local BH mass density appears to be currently active as Seyfert galaxies and the inferred mass accretion rates in such cases are typically 10^3 times lower than in QSOs. This suggests that there *is no significant growth of BHs in the present epoch compared to the quasar era.* Thus, we should bear in mind that local AGN (Seyferts) with current low levels of BH growth may well differ from luminous QSOs near $z \sim 2.5$ in one or more of the following characteristics: *the nature of the dominant fueling mechanism, the amount of cold gas reservoir, and the nature of*

the host galaxy. For instance, tidal interactions and minor or major mergers may have been much more important in the quasar era and early epochs of galaxy growth than they are in activating present-day Seyfert galaxies.

3.5 The Starburst–AGN Connection

While I discuss the fueling of both AGN and starbursts in this review, I will not explicitly address the starburst–AGN connection. I only mention here that this connection can be *circumstantial, influential, or causal.* A *circumstantial* connection refers to the fact that starburst and AGN activity can both manifest in the same system simply because they are affected by a common element such as a rich supply of gas, or an external trigger (e.g., an interaction). Examples include the ULIRG–QSO connection (Sanders et al. 1988), evolutionary scenarios for Seyfert 2 (e.g., Storchi-Bergmann et al. 2001), and perhaps the blue color of AGN hosts described in § 4. An *influential* connection is one where the AGN and starbursts may contaminate each other's *observed* properties. Examples include the starburst affecting the featureless continuum and line ratios of Seyferts (Cid-Fernandes et al. 2001), or washing out the hard accretion disk spectrum. A *causal* connection is a more fundamental connection where the starburst causes the AGN or vice versa. One example is the evolution of a dense stellar cluster into a BH (Norman & Scoville 1988).

3.6 A Note of Caution on Empirical Correlations

There exists many contradictory reports in the literature of correlations or lack thereof between starburst/AGN activity and host galaxy properties (e.g., Hubble types, bar fraction, nuclear bar fraction), or external triggers (e.g., presence of companions, morphological signs of interactions/mergers). Many caveats conspire towards this dismal state of affairs and should be avoided: *(1)* Many early studies fail to adopt the key practice of having a large control sample which is matched to the active sample or to the starburst sample in terms of relevant parameters such as distance, morphological types, luminosities, inclinations, and environments. *(2)* The classification of morphological features such as bars and Hubble types is still often made from optical catalogs (e.g., the Third Reference Catalogue (RC3); de Vaucouleurs et al. 1991) and suffer from subjectivity, low spatial resolution, and contamination by dust. It is better to use a quantitative method (e.g., ellipse fits) for characterizing bars and apply it to near-infrared (NIR) rather than optical images. The former are less affected by extinction and typically yield a bar fraction which is higher by 20–30 % (e.g., Knapen et al. 2000; Eskridge et al. 2002). *(3)* Cross comparisons of discrepant results are often difficult because they are based on inhomogeneous samples drawn from different local AGN catalogs that have limited overlap and different biases. For instance, optically

selected magnitude-limited samples may be biased against faint nuclei embedded in bright galaxies. UV-based catalogs may favor blue Seyfert 1 and quasars. Commonly used catalogs include the Veron-Cetty & Veron Catalog of Seyferts and LINERS, the optically selected CfA sample of 48 Seyferts (Huchra & Burg 1992), the Palomar Optical Spectroscopic Survey (POSS; Ho et al. 1997a) of 486 emission line nuclei geared towards low luminosity HII and AGN nuclei, and the extended 12 μm Galaxy Sample (E12GS) of 891 galaxies (Hunt & Malkan 1999). *(4)* Nuclear types (HII, LINER, Seyferts) listed in literature databases such as NED often show significant discrepancies from recent careful spectroscopic classifications (e.g., Ho et al. 1997a). In § 4–9, I will focus on studies which tend to avoid these caveats or alternatively qualify the caveats as they arise.

4 Hubble Type and Colors of AGN Hosts

Do local Seyferts and central starbursts reside preferentially in certain type of galaxies? Using the 12 μm sample (E12GS) and the CfA sample of Seyferts, Hunt & Malkan (1999; Fig. 3) report that *Sy 1 and Sy 2 nuclei tend to reside primarily in early-type (E–Sbc) galaxies.* The Hubble type quoted here is the RC3 Hubble index based on visual classifications of optical images. A similar result on Seyferts is reported by Ho et al. (1997a) from the POSS optical spectroscopic survey which tends to include lower luminosity galaxies and has a median extinction-corrected Hα luminosity of only 2×10^{39} erg s^{-1}. These findings on Seyferts are consistent with earlier less comprehensive studies (e.g., Hummel et al. 1990; Terlevich, Melnick, & Moles 1987; Balick & Heckman 1982). HII host galaxies tend to have later Hubble types than Seyferts according to both E12GS (Hunt & Malkan 1999) and POSS (Ho et al. 1997a), but the mean value of the Hubble type varies in the surveys, possibly due to luminosity differences.

Properties of AGN hosts in the redshift range 0.5–2.5 are particularly interesting as the optical QSO activity peaks at $z \sim 2.5$. Keen insights are stemming from two large panchromatic *HST* surveys, the Galaxy Evolution from Morphology and SEDs (GEMS; Rix et al. 2004) and the Great Observatories Origins Deep Surveys (GOODS; Giavalisco et al. 2004). A GEMS study of 15 AGN which have $M_B \simeq$ -23 and are in the redshift range $0.5< z <1.1$ where comparable data for control inactive galaxies exist, report that 80% of the AGN hosts are early-type (bulge-dominated) compared to only 20% that are disk-dominated (Sanchez et al. 2004). The high rest-frame *B*-band concentration indices of the GOODS AGN at $z \sim 0.4$–1.3 (Grogin et al. 2004; § 2.2) also support the interpretation that these systems are predominantly bulge-dominated.

Furthermore, Sanchez et al. (2004) report that a much larger fraction (70%) of the early-type AGN hosts at $0.5< z <1.1$ show blue global rest-frame *U-V* colors, compared to inactive early-type galaxies in this redshift and

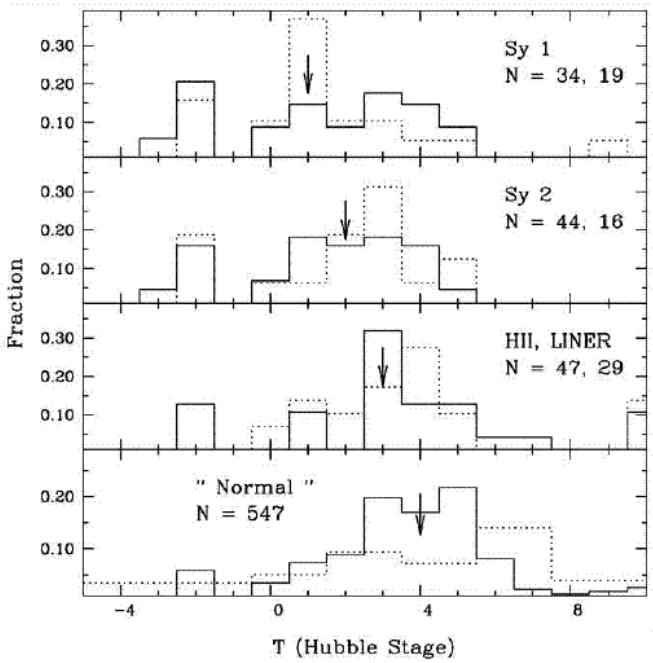

Fig. 3. Distributions of the Hubble types in AGN (Seyferts, LINERS), HII and normal nuclei: The *solid line* in all four panels represents data from the 12 μm sample (E12GS; Hunt & Malkan 1999). The *dotted line* represents data taken from E12GS or other AGN catalogs. The panels represent *(from top to bottom)* (1) The Sy1 sample from E12GS (solid line) and the CfA (dotted line) sample; (2) The Sy1 sample from E12GS (solid) and the CfA (dotted) sample; (3) The HII (solid) and LINER (dotted) samples from E12GS; (4) The normal galaxies from E12GS (solid) and the Uppsala General Catalog (dotted) as tabulated by Roberts & Haynes (1994). The numbers in each panel refer to the number of objects represented by the solid and dotted histograms. The data have been binned in terms of RC3 Hubble types as follows: S0a and earlier ($T >0$); Sa, Sab ($0< T <2$); Sb, Sbc ($2< T <4$); Sc, Scd ($4< T <6$); Sd and later ($T >6$). The vertical arrows mark subsample medians, calculated with a type index resolution of unity. (Figure is from Hunt & Malkan 1999)

luminosity range. These global blue colors are consistent with the presence of young stellar populations over large regions of the AGN host galaxies. The trend of enhanced blue colors in AGN hosts at $0.5< z <1.1$ seems to hold both at higher and lower redshifts. SDSS spectra of local $z < 0.2$ Sy2 galaxies show a significant contribution from young stellar populations, and this trend is strongly correlated with nuclear luminosity (Kauffman et al. 2003). At higher redshifts ($1.8 < z < 2.75$), Jahnke et al. (2004) find that the host galaxies of 9 moderately bright ($M_{\rm B} \simeq$ -23) AGN in the GEMS survey

have rest-frame UV colors that are considerably bluer than expected from an old population of stars. Unfortunately, for these 9 distant AGN the detection images are not deep enough to constrain the morphology. Earlier studies of a handful of luminous QSO at $z > 2$ also reported very UV-luminous hosts (e.g., Lehnert et al. 1992; Hutchings et al. 2002).

One possible interpretation of the enhanced global blue colors exhibited by AGN hosts is that the mechanism which ignites the central BH in these galaxies also triggers global SF. The fact that SF is triggered not only in the nuclear region, but over an extended (several kpc) region, would tend to exclude major (1:1) mergers and favor weaker (e.g., minor (1:10) or intermediate mass-ratio (3:1)) mergers/interactions where the gas has a larger L, and typically settles in extended inner disks during simulations (see § 5). In fact, only 3/15 of the AGN hosts in the Sanchez et al. (2004) study show signs of strong disturbances. In the same vein, the GOODS AGN study (Grogin et al. 2004; § 2.2) reports no significant difference between the rest-frame B asymmetry index of active and inactive galaxies over $z \sim 0.4$–1.3. This suggests that AGN do not preferentially occur in major mergers over this redshift range.

5 Interactions and AGN/Starburst Activity

5.1 Basic Physics of Major Mergers

The term 'major merger' usually refers to the merger of two disk galaxies with a mass ratio of order 1:1. Simulations of major mergers (e.g., Negroponte & White 1983; Noguchi 1988; Barnes & Hernquist 1991; Heller & Shlosman 1994; Mihos & Hernquist 96; Struck 1997) show that they generate large gas inflows into the inner kpc and could plausibly trigger intense starbursts and AGN activity. The full parameter space controlling the outcome of major mergers has not yet been fully explored, but I summarize here (see also Fig. 2) some salient general findings:

1. Not all speeds, energies, angular momenta, and orientations are equally effective in inducing large gas inflows, rapid mergers, and disruptions during a major merger. For instance, while all bound orbits will eventually lead to mergers, low angular momentum and low energy orbits will lead to more rapid mergers. Prograde mergers, where the spin and orbital angular momenta are aligned, occur faster than retrograde mergers, lead to more violent disruption, and excite larger non-circular motions (e.g., Binney & Tremaine 1987).
2. Hydrodynamical torques (shocks) tend to be important in the initial collision when they add spin angular momentum to the gas in both disks (Mihos & Hernquist 1996; Barnes & Hernquist 1996), but gravitational torques dominate thereafter.

3. In the *early stages* of the merger, gas inflows primarily result from *gravitational torques exerted by a stellar bar* induced in the disk of the two galaxies (e.g., Mihos & Hernquist 1996; Heller & Shlosman 1994; Noguchi 1988, Sellwood 1988; Hernquist 1989). The torque from the bar is significantly larger than the gravitational torque exerted by the galaxies on each other. Thus, early gas inflows are primarily the result of gas response in a barred potential as outlined in § 6. Mihos & Hernquist (1996) find that the strength of the bar induced decreases as the bulge-to-disk (B/D) ratio of the disk increases. This behavior is consistent with the idea that a dynamically hot bulge component stabilizes a disk against a bar mode.
4. In the *final stages* of the merger, as the galaxies merge and undergo violent relaxation, the gas experiences rapidly varying gravitational torques as well as shocks on interacting orbits (e.g., Mihos & Hernquist 1996), and therefore loses energy and angular momentum. Large gas inflows ($\gg 1 M_\odot$ yr^{-1}) can result in the late merger stages, provided the episodes of SF triggered by earlier inflows have not depleted most of the gas already. In simulations with highly gas-rich disks (Heller & Shlosman 1994), large gas concentrations build up in the inner kpc leading to the formation of self-gravitating gas clumps which are driven to smaller scales by dynamical friction from the stellar background (see also § 9). Gaseous nuclear bars form via gravitational instabilities and drive further inflow.
5. After violent relaxation, the end-product of a major merger tends to have an $r^{1/4}$ de Vaucouleurs-type stellar profile and boxy isophotes similar to many luminous elliptical galaxies. In the case of intermediate mass ratio (e.g., 1:3) mergers, the gas has a larger specific angular momentum and tends to settle into an extended inner disk (Naab & Burkert 2001) rather than being as centrally concentrated as in a 1:1 merger. The stellar component has an $r^{1/4}$ profile, disky isophotes, and isotropic velocity dispersion similar to lower luminosity disky ellipticals (Naab & Burkert 2001).
6. Future work has yet to fully explore the parameter space which can influence a merger such as the energy and orbital angular momentum of the initial orbits, the relative alignment of the spin and orbital angular momentum, the orbital geometry, the gas content, and the mass ratios. Another key step is to realistically incorporate in simulations feedback effects from SF and thermal cooling effects which lead to a multi-phase ISM (e.g., Struck 1997; Wada & Norman 2001). Shocks from SNe can dissipate orbital energy and transfer angular momentum outwards. Major heating processes associated with SF such as stellar winds, SNe, and UV photoheating are sources of angular momentum, leading to fountain flows and starburst-driven winds (Jogee, Kenney, & Smith 1998; Heckman et al. 1990).

5.2 Basic Physics of Minor Mergers

The term 'minor merger' usually refers to the merger between a large disk galaxy and a satellite with a mass ratio of order 1:10. Such mergers are believed to be very common (Ostriker & Tremaine 1975) and have been the subject of numerous simulations (e.g., Hernquist & Mihos 1995; Mihos et al. 1995; Quinn, Hernquist, & Fullagar 1993; Walker, Mihos, & Hernquist 1996). A few of the general principles underlying this class of mergers are outlined below.

1. As it moves through the dark matter halo, the satellite experiences dynamical friction and sinks rapidly towards the main disk on a timescale $t_{\rm df} \propto (R^2\ v/M\ \ln\Lambda)$, where M is the mass of the satellite, v is its speed, R is the galactocentric radius, and $\ln\Lambda$ is the Coulomb logarithm (Binney & Tremaine 1987). For typical values of these parameters, the dynamical friction timescale is comparable to a few orbital periods or a few Gyr. The orbital angular momentum of the satellite is converted into spin angular momentum for the disk and halo of the main galaxy.
2. The satellite first tends to sink in the disk of the primary where it drives warps before it sinks towards the central regions (Quinn et al. 93; Hernquist & Mihos 1995). Depending on the shape of the halo, these warps can persist for a significant fraction of time before they are washed out by phase mixing (Quinn et al. 93; Dubinski 1994).
3. The satellite exerts tidal torques on the main stellar disk and *induces in it large amplitude non-axisymmetries* (Hernquist & Mihos 1995; Mihos et al. 1995; Quinn et al. 1993) such as stellar spirals and bars. Since gas is collisional and dissipative, the gas response leads the stellar response (see § 6) and gas in the disk is gravitationally torqued towards the central few hundred pc. In effect, *the gas in the main disk experiences a much larger gravitational torque from stars in the disk than from the satellite.* In simulations by Hernquist & Mihos (1995), a large fraction of the gas in the main disk can be driven into the central regions in this way.
4. The satellite may have a significant fraction of its material tidally stripped before it sinks towards the inner part of the main disk.
5. Overall, the minor merger leads to large gas concentrations in the inner few 100 pc which may be relevant for fueling starbursts and AGN. It also heats the inner parts of disks vertically and increases the disk thickness and velocity dispersion of stars. Some authors (e.g., Quinn et al. 1993; Walker et al. 1996) have even suggested that minor mergers may be the origin of thick disks.

5.3 Correlations between Interactions and Starbursts

Colorful examples abound of starbursts and AGN activity occurring in interacting or merging galaxies. However, statistically significant correlations

between central activity and signs of morphological disturbance have only been found in the case of highly luminous starbursts or AGN. Signs of strong tidal interactions and mergers are ubiquitous in systems where the SR rate (SFR) is estimated to be $\geq 10\,\mathrm{M}_{\odot}\,\mathrm{yr}^{-1}$ such as ultra-luminous infrared galaxies (ULIRGs; Veilleux, Kim, & Sanders 2001; Sanders & Mirabel 1996), and the brightest Arp galaxies (Hummel et al. 1990; Kennicutt et al. 1987). In the local Universe, more than 95% of ULIRGS in the 1 Jy IRAS sample show optical and NIR morphological signatures of a strong interaction or merger in the form of tidal tails, bridges, double nuclei, and overlapping disks (Veilleux et al. 2001). In a study based on panchromatic *HST* GOODS data, optically-selected bright starburst galaxies at $z \sim 1$ show a larger frequency ($\sim 50\%$) of disturbed and asymmetric morphologies, compared to 13% and 27%, respectively, in control samples of early-type and late-type galaxies (Jogee et al. 2003; Mobasher et al. 2004).

While the most extreme *individual* starbursts (in terms of luminosity or luminosity per unit mass of gas) may be triggered by a major or intermediate mass ratio interaction, it is important to bear in mind that the *cumulative* SFR density at a given cosmic epoch may be dominated by SF emanating from a large number of relatively undisturbed galaxies rather than from SF in major mergers. This is a particularly viable possibility out to intermediate redshifts ($z \sim 1$) where major mergers are relatively rare. In fact, preliminary findings (Wolf et al. in prep.) from a study of ~ 1400 galaxies at $z \sim 0.7$ in the GEMS survey suggest that while galaxies with strongly disturbed rest-frame optical morphologies are amongst the most UV-luminous candidates, they only make up a small fraction of the UV luminosity density (uncorrected for extinction) at $z \sim 0.7$. While this result on UV luminosity density does not directly translate to SFR density due to potential extinction effects, it does highlight the need for further studies on how mergers/interactions impact central activity.

5.4 Correlations between Interactions and AGN

An excess of companions in local Seyferts has been reported in early papers (e.g., Dahari 1984; Keel et al. 1985), but more recent studies with large or/and well-matched control samples show no strong correlations (e.g., Schmitt 2001; Laurikainen & Salo 1995). Furthermore, in a study of 69 galaxies belonging to 31 Hickson compact groups (CGs), Shimada et al. (2000) find no difference between the frequency of HII or AGN nuclei in Hickson CGs and field galaxies.

At intermediate redshifts ($z \sim 0.4$–1.3), studies based on GOODS data (Grogin et al. 2004; see § 2.2) report no significant difference between the rest-frame B asymmetry index of AGN hosts and inactive galaxies. This suggests that over this redshift range, AGN hosts are not preferentially major mergers. Similarly, in the GEMS sample of moderately bright ($M_{\mathrm{B}} \simeq$ -23) AGN at $0.5 < z < 1.1$ studied by Sanchez et al. (2004; see § 4), only 3/15 of the AGN

hosts signs of strong disturbances, and at most three others are associated with nearby potentially interacting companions.

In fact, statistically significant correlations between AGN activity and signs of strong interactions are reported only in systems with high mass accretion rates ($\geq$ 10 $M_\odot$ yr^{-1}) such as very luminous or radio-loud QSOs (Disney at al. 1995; Bahcall et al. 1997; Kirhakos et al. 1999), and FR-II radio galaxies (Hutchings 1987, Yates et al. 1989). I discuss below possible reasons as to why a correlation is only seen at the very high luminosity end:

- It is possible that the large mass accretion rates ($\geq$ 10 $M_\odot$ yr^{-1}) on small scales required by very high luminosity QSOs are realized in nature primarily during violent processes such as some classes of major/intermediate mass-ratio interactions. In particular, the last phases of a major merger produce rapidly varying gravitational torques and strong shocks on intersecting orbits (see § 5.1) that are expected to generate large inflow rates on small scales.
- Conversely, in order to fuel Seyferts over their nominal duty cycles (10^8 years) with a mass inflow rates $\leq$ 0.01 $M_\odot$ yr^{-1}), any one of the many 10^6 $M_\odot$ clouds commonly present within the inner 200 pc radius is adequate, provided that some fueling mechanism drains its angular momentum by more than 99.99% (Fig. 2). Given that the required fueling mass is 10^{-3}–10^{-2} of the amount of gas typically found in the inner few 100 pc, it is well possible that *localized* low-energy processes (e.g., SNe shocks on ambient clouds) may be adequate for reducing its angular momentum. In other words, interactions and other fueling mechanisms which affect the *bulk* of the gas may not be necessary for fueling Seyferts.

6 Large-Scale Bars in Starbursts/AGN Hosts

6.1 Bar-Driven Gas Inflow: Theory and Observations

Bars are ubiquitous in most ($>$ 70%) local spiral galaxies (Grosbøl et al. 2002; Eskridge et al. 2002), and recent work (Jogee et al. 2004a,b; Sheth et al. 03) suggest they may be quite abundant out to $z \sim 1$. Bars drive the dynamical evolution of disk galaxies by exerting gravitational torques which redistribute mass and angular momentum. In fact, large gas inflows into the inner few hundred pc of a disk galaxy primarily result from gravitational torques exerted by a stellar bar. This is true not only in the case of an isolated barred galaxy, but also for some classes of minor mergers (§ 5.2; Quinn et al. 1993; Hernquist & Mihos 1995; Mihos et al. 1995), most intermediate 1:3 mass ratio mergers (Naab & Burkert 2001), and the early phases of most major mergers (§ 5.1; Noguchi 1988, Sellwood 1988; Hernquist 1989; Heller & Shlosman 1994; Mihos & Hernquist 1996). I will, therefore, devote a fair share of this review to a discussion of the basic principles of bar-driven gas

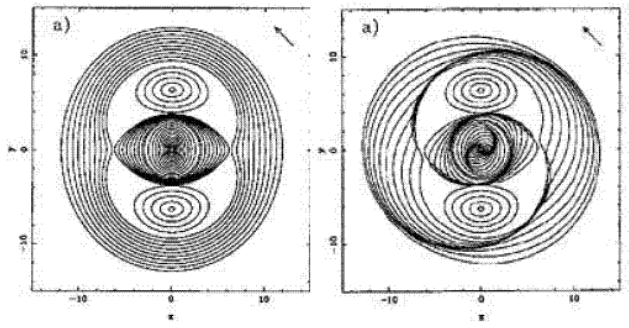

Fig. 4. Stars and gas in a barred potential: *Left:* The periodic *stellar* orbits in the potential of a bar (oriented horizontally here) change orientation by $\pi/2$ at each resonance. The x_1 family of periodic stellar orbits is elongated along the bar major axis and supports the bar. The x_2 orbits are elongated along the bar minor axis and and exist inside the ILR or between the ILRs. *Right:* In contrast, gas being collisional and dissipative, follows orbits which change their orientation only gradually, leading to spiral-shaped gas streamlines. (Figures are adapted from Buta & Combes 1996)

inflow, what it can achieve in the context of fueling starbursts and AGN, and related observations.

A barred potential is made up of different families of periodic stellar orbits which conserve the Jacobi integral ($E_{\rm J}$), a combination of energy and angular momentum (e.g., Binney & Tremaine 1987). The most important families are those oriented parallel to the bar major axis (x_1 orbits; Contopoulos & Papayannopoulos 1980) and minor axis (x_2 orbits). The x_1 family is the main family supporting the bar and extends between the center and the corotation resonance (CR) of the bar. The inner Lindblad resonances demarcate the transition region where the dominant family of periodic stellar orbits changes from x_1 to x_2. Thus, the x_2 family appears between the center and the ILR if a single ILR exists, and between the inner ILR (IILR) and the outer ILR (OILR) if two ILRs exist. Gas tries to follow these orbits, but due to its collisional and dissipative nature, it cannot remain on periodic orbits which cross. Instead, the gas-populated orbits change their orientation only gradually due to shocks induced by the finite gas pressure, leading to spiral-shaped gas streamlines, offset with respect to the stars (Fig. 4). The negative torque exterted by the stars between CR and the OILR causes the gas to lose angular momentum and flow towards the inner kpc.

There is mounting observational evidence for bar-driven gas inflow into the inner kpc. Moderate ($4''$) resolution CO(J=1–0) interferometric surveys of molecular gas in the circumnuclear region of nearby spirals show that the molecular gas central concentration (Fig. 5) is on average higher in barred than in unbarred galaxies (Sakamoto et al. 1999). Barred galaxies also show

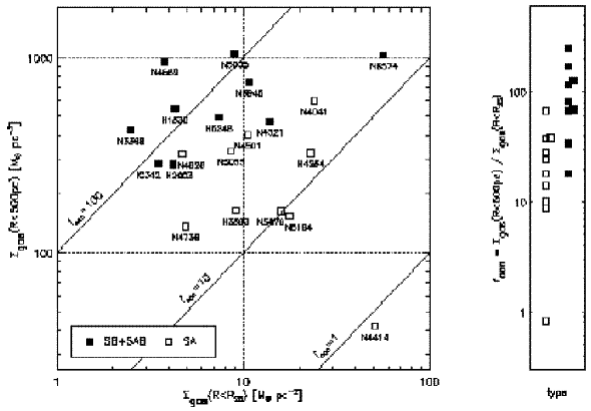

Fig. 5. Molecular gas central concentrations in barred galaxies: *Left:* Comparison of the molecular gas surface densities averaged within the central 500 pc radius and over the optical de Vaucouleurs radius (R_{25}). The spatial resolution of the data is $\sim$ 4″. The ratio of these two quantities is a measure of the molecular gas central concentration ($f_{\rm con}$) within the central kpc. *Right:* On average the molecular gas central concentration ($f_{\rm con}$) within the central kpc is higher in barred galaxies (filled squares) than in unbarred galaxies (open squares). (Figure is adapted from Sakamoto et al. 1999)

shallower metallicity gradients across their galactic disks than unbarred ones (Martin & Roy 1994; Vila-Costas & Edmunds 1992). Observations of cold or ionized gas velocity fields show evidence for shocks and non-circular motions along the large-scale stellar bar (Quillen et al. 1995; Benedict, Smith , & Kenney 1996; Regan, Vogel, & Teuben 1997; Jogee 1999; Jogee, Scoville, & Kenney 2004c). Bar-driven gas inflow rates into the inner kpc have been estimated only in the case of a few strong bars and range from 1 to 4 $M_\odot$ yr^{-1} (Quillen et al. 1995; Regan et al. 1997; Laine, Shlosman, & Heller 1998).

What happens once gas reaches the central kpc region of barred galaxies? High resolution (1–2″; 100-200 pc) observations of molecular gas and SF in the central few kpc of eleven barred galaxies (Jogee et al. 2004c; Fig. 6) reveal a variety of gas distributions and a large range in SFR per unit mass of molecular gas (SFR/$M_{\rm H2}$). These differences in gas distributions and SF efficiencies can be partly understood in terms of different stages of bar-driven inflow and the existence of a critical density for the onset of SF (Jogee et al. 2004c). Some systems appear in the early stages of bar-driven inflow where a large fraction of the gas is still extended along the large-scale bar, shows large non-circular kinematics and does not form stars efficiently. Other galaxies have developed large gas surface densities (600-3500 $M_\odot$ pc^{-2}; Fig 7) inside

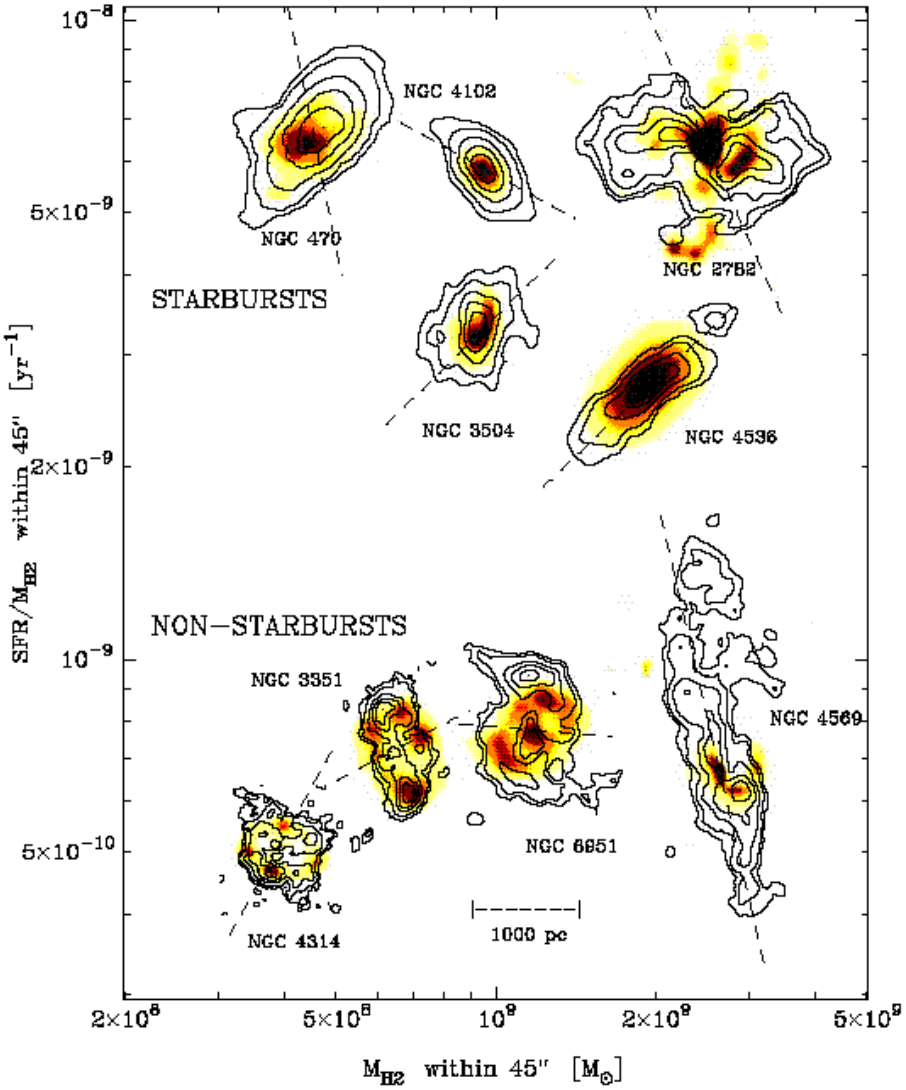

Fig. 6. High resolution (2″ or 100–200 pc) observations of molecular gas and star formation in the inner few kpc of barred galaxies: CO (1–0) intensity (contours) maps of the circumnuclear region of barred galaxies are overlaid on 1.5 or 4.9 GHz radio continuum map or Hα map (greyscale). The dotted line is the P.A. of the large-scale stellar bar/oval. A wide range in gas distributions and in SFR per unit mass of molecular gas (SFR/$M_{\rm H2}$) is present. Systems with high/low circumnuclear SFR/$M_{\rm H2}$ are denoted as starbursts/non-starbursts. Part of the range in SFR/$M_{\rm H2}$ and the variety of gas distributions can be understood in terms of different stages of bar-driven inflow and the critical density for the onset of SF. (From Jogee et al. 2004c; see text for details).

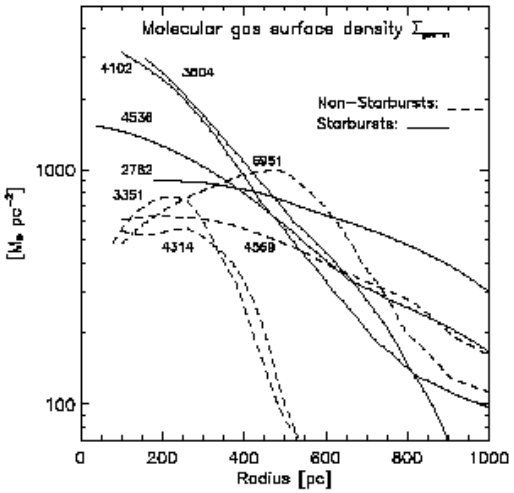

Fig. 7. Molecular gas surface densities in the inner kpc of barred galaxies: The azimuthally averaged molecular gas surface density derived from the high resolution ($2''$ or 100–200 pc) CO (J=1–0) maps in Fig. 6 are plotted. Quantities are plotted starting at a radius $\geq$ half the size of the synthesized beam. Most of the starbursts have developed larger molecular gas surface densities (1000-3500 $M_{\odot}$ pc^{-2}) in the inner 500 pc radius than the non-starbursts for a given CO-to-H_2 conversion factor. (From Jogee et al. 2004c)

the OILR of the bar. Intense starbursts appear to be triggered only once gas densities approach or exceed the Toomre critical density for the onset of gravitational instabilities (Elmegreen 1994; Jogee et al. 2004c).

While the large-scale bar efficiently drives gas from the outer disk into the inner kpc, theory suggests that the radial inflow of gas slows as it crosses the ILR because shocks associated with the large-scale bar weaken, the gravitational potential becomes more axisymmetric, and gravitational torques on the gas in the vicinity of ILRs weaken or even reverse (e.g., Schwarz 1984; Combes & Gerin 1985; Shlosman et al. 1989; Athanassoula 1992). In support of this picture, gas rings near the ILRs have also been reported in many individual galaxies (e.g., Kenney et al. 1992; Knapen et al. 1995; Jogee 1999; Jogee et al. 2001). Figure 8 illustrates the results from high resolution observations of gas in the centers of barred galaxies (Jogee et al. 2004c). In the seven barred galaxies shown, typically the OILR radius is $\geq$ 500 pc while the IILR radius is $\leq$ 200–300 pc. It should be noted that even with these high resolution (100 pc) data, it remains difficult to assess the presence/response of gas *inside* the IILR since the latter radius is comparable to the spatial resolution.

The question of whether bars are long-lived or whether they dissolve and reform recurrently over a Hubble time is highly controversial at the present

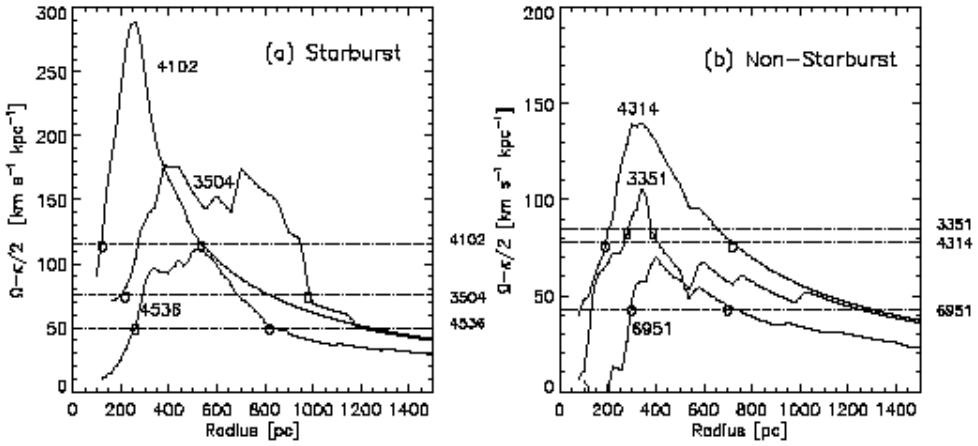

Fig. 8. Location of Inner Lindblad resonances in barred galaxies: [Ω - $\kappa/2$] is plotted against radius for the circumnuclear region of the barred galaxies shown in Fig 6. Under the epicyclic approximation valid for weak bars, the intersection of [Ω - $\kappa/2$] with $\Omega_{\rm p}$ defines the locations of the ILRs of the large-scale stellar bar. The upper limit on the bar pattern speed ($\Omega_{\rm p}$) is drawn as a horizontal line and is estimated by assuming that the corotation resonance is at or beyond the bar end. Values range from 43 to 110 km s^{-1} kpc^{-1}. Typically, the OILR radius is $\geq$ 500 pc while the IILR radius is $\leq$ 200–300 pc. Thus, in these systems, the large molecular gas densities (Fig. 5) have developed inside the OILR of the bar/oval. (From Jogee et al. 2004c)

time. Early studies (Hasan & Norman 1990; Friedli & Benz 1993; Norman, Sellwood, & Hasan 1996, but see also Bournaud & Combes 2002; Shen & Sellwood 2004) proposed that once a large central mass concentration (CMC) builds up in the inner 100 pc of a galaxy, it will destroy or weaken the bar due to the development of chaotic orbits and reduction of bar-supporting orbits. In some scenarios, bars even cause their own demise and self-destruction by building up such CMCs via gas inflows. The disk left behind after a bar is destroyed is dynamically hot and does not reform a new bar unless it is cooled significantly. Recently, Bournaud & Combes (2002) suggested that bars are destroyed primarily due to the reciprocal torques of gas on the stars in the bar (rather than by the CMC *per se*). Within this framework, bars can dissolve and reform recurrently if the galaxy accretes sufficient cold gas over a Hubble time. In fact, Shen & Sellwood (2004) find that in purely stellar N-body simulations, the bar is quite robust to CMCs. Ongoing studies (Jogee et al. 2004a,b) of the bar properties and CMCs of galaxies over lookback times of 9 Gyr (out to $z \sim 1$), based on the GEMS survey, will help provide discriminant tests on the evolution and lifetime of bars out to $z \sim 1$.

6.2 Correlations between Large-Scale Bars and Starbursts

Analyses of the extended 12 μm Galaxy sample (E12GS) show that the fraction of large-scale bars is larger in starburst nuclei (82–85%) than in normal (61-68%) ones (Fig 9; Hunt & Malkan 1999). The term 'normal' here denotes quiescent nuclei which do not have HII/starburst, LINER, Sy 1, or Sy 2 signatures. Similar correlations between large-scale bars and circumnuclear starbursts were previously reported by studies with smaller or/and less complete samples. For instance, Hawarden et al. (1986) found that a large fraction of SB and SAB galaxies show an enhanced IRAS 25 μm flux, which they assigned to circumnuclear rings of SF present in the central 20″. Earlier work (e.g., Terlevich et al. 1987; Kennicutt et al. 1987) also reported correlations based on UV and optical starbursts.

All the afore-described studies rely on optical images to identify bars and therefore suffer from the associated caveats outlined in § 3.6. Taken at face value, they suggest that relatively luminous starbursts have a higher frequency of large-scale stellar bars than normal galaxies. A natural explanation exists for the bar–starburst correlation. The most powerful starbursts typically occur in the central few 100 pc of galaxies once large supercritical gas densities (often as large as several 1000 $M_\odot$ pc^{-2}; Jogee et al. 2004c) build up. A spontaneously or tidally induced large-scale bar is an ideal fueling mechanism for luminous circumnuclear starbursts because it efficiently drains angular momentum from gas on exactly the right spatial scales (several kpc to a few hundred pc; Fig 2) relevant for building the pre-requisite large concentrations.

6.3 Correlations between Large-Scale Bars and AGN

The study of Hunt & Malkan (1999) based on the E12GS sample and RC3 optical bar classes finds that there is no excess of bars in Seyferts. Two recent NIR-based studies (Mulchaey & Regan 1997; Knapen et al. 2000) have investigated the fraction f of large-scale bars in Seyferts and normal galaxies using matched control samples, high resolution NIR images, and ellipse fits to characterize bars. Mulchaey & Regan (1997) report a similar incidence of bars ($f \sim 70\%$) in Seyferts and normal galaxies while Knapen et al. (2000) find a higher fraction of bars in Seyferts ($79\% \pm 8\%$ vs. $59\% \pm 9\%$) at a significance level of 2σ. More recently, Laurikainen, Salo, & Buta (2004) classified bars in the Ohio State University sample (Eskridge et al. 2002) using Fourier decomposition of NIR images (Fourier bars), and report a higher fraction (72%) of such Fourier bars in Seyfert galaxies, LINERs, and HII/starburst galaxies, as compared to 55% in the inactive galaxies. It is not entirely clear at this time how the Fourier bars identified in this study compare to bars identified by other methods such as ellipse fits, and how they are impacted by other m=2 modes (e.g., spirals). Furthermore, the nuclear types (HII, Seyfert, and LINERs) in the OSU sample are not homogeneously

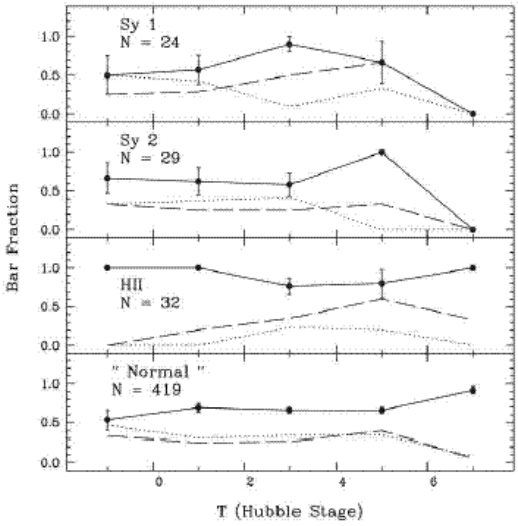

Fig. 9. Relation between large-scale bars and nuclear starburst/AGN: The fraction of barred galaxies as a function of Hubble type and nuclear types is shown for the extended 12 μm Galaxy Sample. Nuclear types (HII, Sy 1, Sy 2, LINER) are taken from NED. Quiescent nuclei without any of these signatures are denoted as 'normal'. Optically-based RC3 bar classes are shown as dotted lines (unbarred), dashed lines (weakly barred SAB), and solid lines (weakly and strongly barred SAB+SB). The data bins are as in Fig. 3. Numbers under the panel label give the number of galaxies in each subsample. (Fig. is from Hunt & Malkan 1999)

classified via spectroscopic observations. Thus, it is fair to conclude that at this time, the question of whether Seyferts have an excess of large-scale bars compared to inactive galaxies remains open.

I discuss below what one might expect with regards to correlations between Seyferts and large-scale bars, based on theoretical considerations, and outline some areas where future work is needed.

1. The first question one might ask is whether all barred galaxies are expected to show AGN activity. It is clear from Fig. 2 and preceding discussions that a large-scale bar efficiently drives gas only down to scales of a few 100 pc. At that stage, the specific angular momentum L of the gas is still 1000 times too high to be digestible by a BH. Thus, unless other mechanisms are present to reduce L further, the gas will not fuel the central BH. Furthermore, even if a barred system does go through an AGN phase, the lifetime of a bar is expected to be at least 1 Gyr, while a typical AGN duty cycle is 10–100 times shorter. *Thus, we do not expect all barred galaxies to show AGN activity.*

2. A different question is whether we would expect all local Seyfert host galaxies to have a bar. This question is tantamount to asking whether we need to transport gas from the outer regions (several kpc) to the inner few 100 pc of a galaxy in order to *directly or indirectly* fuel Seyferts. Let us first consider the required mass budget. The mass of gas required to fuel a typical Seyfert at a rate of 10^{-2} $M_\odot$ yr^{-1} over a nominal duty cycle of 10^8 years is *only 10^6 $M_\odot$ or 10^{-3}–10^{-2} of the typical gas content* (10^8–10^9 $M_\odot$)
found in the inner kpc of a present-day spiral. One might argue, therefore, that we would not expect a strong correlation between Seyfert activity and strong/moderate bars because even weak/inefficient large-scale fueling mechanisms are more than adequate to drive such tiny amounts of gas from kpc scales down to the inner few 100 pc. Examples of such weak fueling mechanisms would be oval features which are not conventionally classified as bars, weak non-axisymmetries easily induced in minor mergers/interactions, and dynamical friction slowly sinking a gas-rich satellite (see § 5.1). It has in fact been argued that the strong excess of rings seen in Seyferts (see point 4) represent such weal oval perturbations. In summary, from the point of view of *large-scale gas transport,*one would not expect strong/moderate large-scale bars to be a pre-requisite for fueling Seyferts.
However, we should bear in mind that a correlation between Seyfert and strong/moderate large-scale bars might *indirectly* result due to requirements for gas transport on *small* scales (100s of pc) rather than large (kpc) scales. Even if only 0.1%–1% of the gas present on scales of a few 100 pc provides an adequate mass budget for AGN activity over many duty cycles, the fueling of the BH can only occur if there exist mechanisms on scales of a few 100 pc which can drain the angular momentum of this gas by more than 99.99%. If some of these mechanisms, such as dynamically decoupled secondary nuclear bars, are favored by the presence of a moderate/strong large-scale bar, a correlation between the latter and Seyferts might result. However, one may also counter-argue that with only 0.1%–1% of the circumnuclear gas present being involved in AGN fueling, strong nuclear fueling mechanisms such as nuclear bars may not be needed. Instead, localized low-energy processes such as SNe shocks and cloud-cloud collisions may be enough to significantly reduce the angular momentum on one ambient 10^6 $M_\odot$ cloud and drive it from 100s of pc down to tens of pc.
3. The uncertain question of whether bars can self-destroy and reform recurrently over a Hubble time (see § 6.1) adds another pertinent dimension to the interpretation of statistical correlations or lack thereof between bars and Seyferts. In some models of bar destruction (e.g., Hasan & Norman 1990; Friedli & Benz 1993; Norman, Sellwood, & Hasan 1996), a bar which dutifully brings a large gas concentration into the inner kpc

might dissolve away once other mechanisms in the inner kpc start to relay the fuel to 100 pc scales and eventually to the BH. Some observational support for this picture comes from studies reporting that the bar strength is weaker in Seyferts than in inactive galaxies (Shlosman et al. 2000; Laurikainen et al. 2004).

4. A strong correlation is seen between Seyferts and the presence of large-scale rings in the host galaxies (Hunt & Malkan 1999): the frequency of outer rings and of (inner +outer) rings is higher by 3-4 times in Seyfert galaxies compared to normal galaxies. It has been argued that this correlation may result by chance because both Seyferts and rings (particularly outer rings) tend to be more common in early-type systems. Another possibility is that these oval rings represent the type of weak non-axisymmetric distortions discussed in point 2. A third possibility is that a large fraction of these rings might be remnants of bar dissolution. Both latter possibilities need to be explored further theoretically and observationally.
5. To date, all studies between AGN and large-scale bars have focused on local galaxies. Yet, AGN activity is known to increase with redshift, with the optically bright QSO phases peaking at $z \sim 2.5$ (§ 3.4). It is important to extend studies of bars and AGN to earlier epochs. The ongoing work on the impact and evolution of bars over the last 9 Gyr (out to $z \sim 1.3$) based on the GEMS *HST* survey and Chandra Deep Field South data (Jogee et al. 2004a,b) will help constrain how bars relate to AGN activity at these epochs.

7 Nuclear Bars

7.1 Nuclear Bars: Theory and Observations

A large-scale bar efficiently drives gas from the outer disk down to scales of a few hundred pc where the gas inflow stalls after crossing an ILR. Theory and simulations (Shlosman et al. 1989; Friedli & Martinet 1993; Heller & Shlosman 1994; Maciejewski & Sparke 2000) have suggested that a nuclear bar (so called 'secondary' bar) nested within the large-scale bar (so called 'primary' bar) can break the status quo and gravitationally torque digestible fuel closer to the galactic center. Several scenarios exists for the formation and evolution of nuclear bars. The nuclear bar can decouple from the primary bar such that its pattern speed ($\Omega_{\rm n}$) is higher (Shlosman et al. 1989; Friedli & Martinet 1993; Heller & Shlosman 1994) or lower (Heller, Shlosman & Englmaier 2001) than the primary pattern ($\Omega_{\rm p}$), depending on whether it forms via a self-gravitational or non-self-gravitational instability. The nuclear bar can also be in a coupled phase with ($\Omega_{\rm n}$= $\Omega_{\rm p}$), while in the case of a merger remnant it may even counter-rotate with respect to the primary bar.

In simulations, the decoupled phase with $\Omega_{\rm n} > \Omega_{\rm p}$ is particularly effective in removing angular momentum from the gas and in helping to fuel the BH.

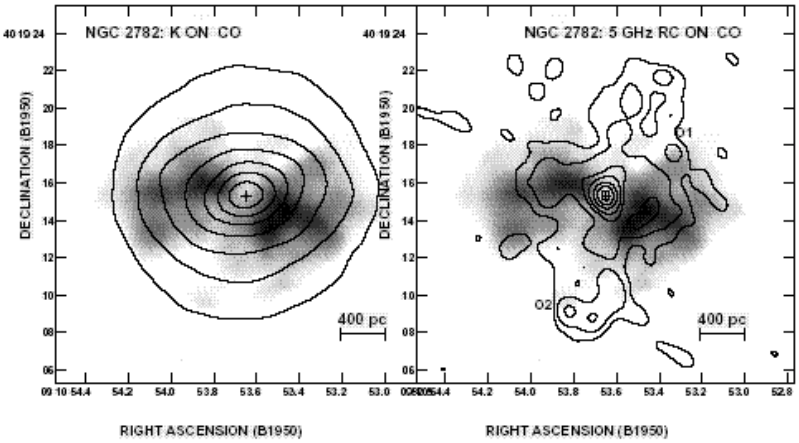

Fig. 10. A nuclear stellar bar feeding gas into a powerful starburst within the inner 100 pc radius of NGC 2782: *Left:* K-band contours are overlaid on the ($2.1'' \times 1.5''$) CO intensity map (greyscale). A nuclear stellar bar (identified via isophotal fitting of the K-band image) is present at a PA of $\sim$ 100 °and is itself nested within a large-scale oval/bar which is visible in a larger I-band image. The cold gas traced in CO has a bar-like distribution which leads the nuclear stellar bar, and its velocity field (not shown here) reveals weak bar-like streaming motions. *Right:* 5 GHz radio continuum (contours) are overlaid on the CO map (greyscale). The nuclear stellar bar appears to be feeding molecular gas into an intense starburst which peaks in RC within the inner 100 pc radius and has a SFR of 3–6 $M_\odot$ yr^{-1}. The starburst in turn appears to be driving an outflow associated with the northern and southern RC bubbles. (From Jogee, Kenney, & Smith 1999)

Most observational studies on nuclear bars have focused on the *morphological* properties of bars determined from optical and IR images (Wozniak et al. 1995; Friedli et al. 1996; Mulchaey & Regan 1997; Jogee, Kenney, & Smith 1999; Laine et al. 2002; Erwin & Sparke 2002; Erwin 2004). Studies using space-based and ground-based IR and optical images reveal that about 20%–30% of S0-Sc galaxies host double bars and 20%–40% of barred galaxies host a second bar (e.g., Laine et al. 2002; Erwin & Sparke 2002). Confirmed morphologically-identified double bars exist primarily in galaxies of Hubble type no later than Sbc. They have ellipticities of 0.27–0.6, semi-major axes of 200–1600 pc, and position angles which both lead and trail the primary bar by varying amounts. The latter fact suggests that a significant fraction of nuclear bars must be dynamically decoupled with respect to the primary bar.

NGC 2782 provides a nice observational case of a nuclear bar driving gas down to 100 pc scales. It hosts a nuclear stellar bar which is associated with $\sim 2.5 \times 10^9$ $M_\odot$ of molecular gas and appears to be channeling gas into the central 100 pc where an M82-class powerful central starburst resides (Fig. 10; Jogee, Kenney, & Smith 1999). The nuclear stellar bar is identified via isophotal fits to K-band image showing a characteristic plateau in position angle (PA) as the ellipticity rises to a maximum. The molecular gas distribution is bar-like, leads the nuclear stellar bar, and shows weak bar-like streaming motions (Jogee et al. 1999). NGC 2782 may be witnessing the early decoupling phase of a nuclear stellar bar induced by gas inside the OILR of the large-scale bar, which itself appears to be dissolving.

Aside from NGC 2782, only a handful of other nuclear bar candidates have high resolution CO maps. These show a wide range of CO morphologies in double-barred galaxies. The double-barred galaxy NGC 5728 shows CO clumps in a very disordered configuration (Petitpas & Wilson 2003). In NGC 4314, the CO emission forms a clumpy ring at the end of the nuclear bar (Benedict et al. 1996; Jogee et al. 2004c). The differences in CO distributions in these nuclear bars may be linked to evolutionary differences (Jogee et al. 2004c) or differences in gas properties (Petitpas & Wilson 2003).

7.2 Correlations between Nuclear Bars and AGN

Multiple investigations have searched for a nuclear bar–AGN correlation. Statistics from earlier studies which used offset dust lanes to identify nuclear bars (e.g., Regan & Mulchaey 1999; Martini & Pogge 1999) must be re-evaluated because simulations (Maciejewski et al. 2002; Shlosman & Heller 2002) show that the gas flow in nested nuclear bars differs fundamentally from that along large-scale bars and does not lead to large-scale *offset* shocks and dust lanes. More recent studies based on isophotal fits to NIR images report that the fraction of nuclear bars is similar (20%–30%) in Seyfert and non-Seyfert hosts (Laine et al. 2002; Erwin & Sparke 2002). There are several possible explanations for the lack of statistical correlations observed between nuclear bars and AGN activity.

1. Nuclear bars help to solve the angular momentum problem one step further than large-scale bars, but the gas still has to lose several orders of magnitude in L even at pc scales (see Fig. 2).
2. Not all morphologically-identified nuclear bars are expected to be equally effective in removing angular momentum from the gas. Theoretically, the most effective ones are those with $\Omega_{\rm n} > \Omega_{\rm p}$. However, to date limited observations exist on *kinematic properties* and pattern speeds of nuclear bars, and this is an area where much progress has yet to be made.
3. Once large mass concentrations build in the core of the nuclear bar, it can cause first the nuclear bar, then the large-scale primary bar, to dissolve. The lifetime of secondary nuclear bars is not precisely determined, but is expected to be short and $\sim$ a few bar rotation timescales.

4. As discussed in § 6.3, only 10^6 $M_\odot$ or 0.1%–1% of the gas present on scales of a few 100 pc can adequately fuel a Seyfert over a nominal duty cycle of 10^8 years at a rate of 10^{-2} $M_\odot$ yr^{-1}. Thus, in lieu of strong fueling mechanisms such as nuclear bars, localized processes such as SNe shocks and cloud-cloud collisions may be adequate for driving one ambient 10^6 $M_\odot$ cloud from 100s of pc down to 10s of pc (see § 6.3 point 2).

8 Nuclear Spirals and AGN/Starburst Activity

There is mounting evidence from high resolution ground-based and *HST* observations of galaxies that nuclear dust spirals are common on scales of a few tens to hundreds of pc (e.g., Elmegreen et al. 1998; Carollo, Stiavelli, & Mack 1998; Laine et al. 1999; Regan & Mulchaey 1999; Martini & Pogge 1999 ; Jogee et al. 2002; Martini et al. 2003). A variety of nuclear spirals are present, including flocculent, chaotic, and two-armed grand-design spirals. Nuclear dust spirals are likely to trace shocks since their arm-to-interarm contrast (Martini & Pogge 1999; Elmegreen, Elmegreen & Eberwein 2002; Laine et al. 1999) implies a mass density enhancement ≥ 2. Since shocks dissipate orbital energy and lead to the outward transfer of angular momentum, some authors have suggested that nuclear dust spirals may play some role in the fueling of AGN.

How do nuclear dust spirals form? Most of them are believed to be in non-self-gravitating central gaseous disks based on the lack of significant SF observed in the spirals. This belief is corroborated in a few cases by rough estimates of the neutral gas mass density Σ(H) and Toomre Q values associated with the nuclear dust spirals (Martini & Pogge 1999). In such a non-self-gravitating gas disk, nuclear spirals may form in several ways. **(1)** Hydrodynamical simulations (Englmaier & Shlosman 2000) suggest that bar-driven shocks which exist near the ILRs can trigger gaseous SDWs which propagate inwards across the ILRs, and lead to grand-design two-armed nuclear dust spirals. Observational support for the model comes from detailed comparisons of the simulations with the data in NGC 5248 (Jogee et al. 2002b; Fig. 11) which hosts a grand-design nuclear spiral. **(2)** Repeated compression from acoustic turbulence followed by shearing can lead to flocculent nuclear dust spirals (Elmegreen, Elmegreen, & Eberwein 2002; Montenegro et al. 1999). **(3)** Simulations including gas dynamical effects (rotation, shear, shocks), thermal cooling effects, and feedback from SF (e.g., Wada & Norman 2001) lead to a multi-phase ISM where chaotic and flocculent spirals reccur.

Is there a correlation between nuclear spirals and AGN activity? A survey based on NIR *HST* images and color maps of 123 nearby galaxies by Martini & Pogge (2003) reports that nuclear dust spirals occur with comparable frequency in both active and inactive galaxies (Fig. 12). This suggests that the low level inflow rate on scales of 10s of pc which might be triggered by shocks in the nuclear spirals is not a universal mechanism for feeding even

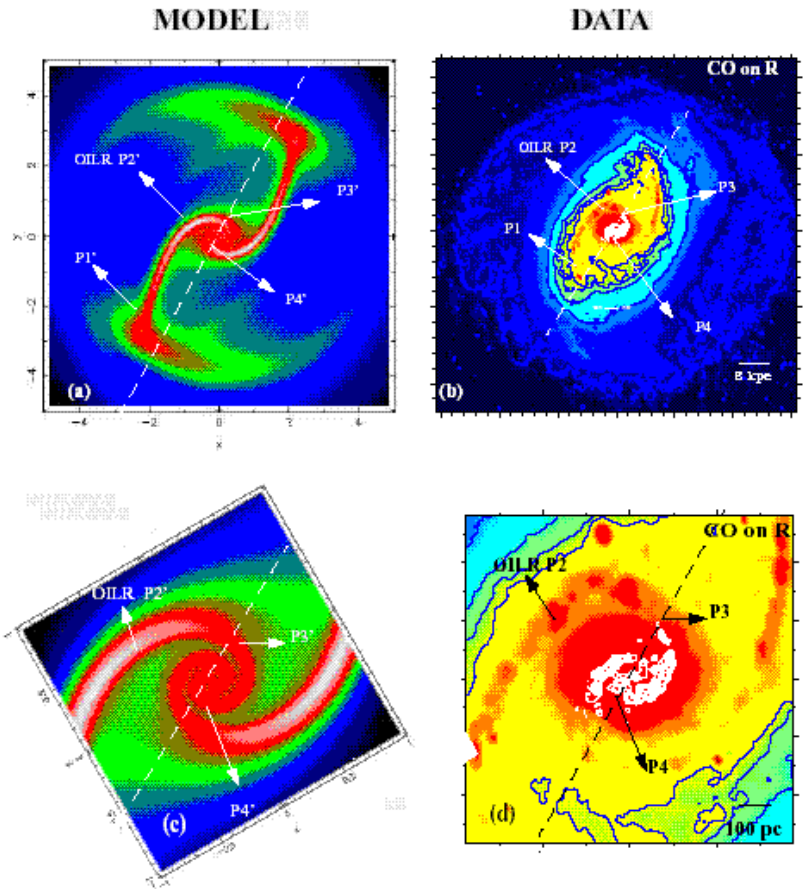

Fig. 11. Bar-driven gaseous spiral density waves (SDWs) forming a grand-design nuclear dust spiral well inside the OILR of NGC 5248: Comparison of the CO and *R*-band data (right) with hydrodynamical models (left; from Englmaier & Shlosman 2000) of a bar-driven gaseous SDW. Points P1' to P4' in the models correspond to points P1 to P4 in the data. The *top* panel shows the entire galaxy, and the *bottom* panel the central 40″ (3.0 kpc) only. In NGC 5248, continuous spirals in CO and dust extend inwards from 6 kpc, cross the OILR (P2) of the bar, continue inwards (P3, P4), and connect to nuclear dust spirals which extend from 300 pc to 70 pc. Comparison of the data with the hydrodynamical models suggest that the continuous connected spiral structure is generated by a gaseous SDW which is driven by the large-scale bar and penetrates very deep inside the OILR due to the low central mass concentration (From Jogee et al. 2002b).

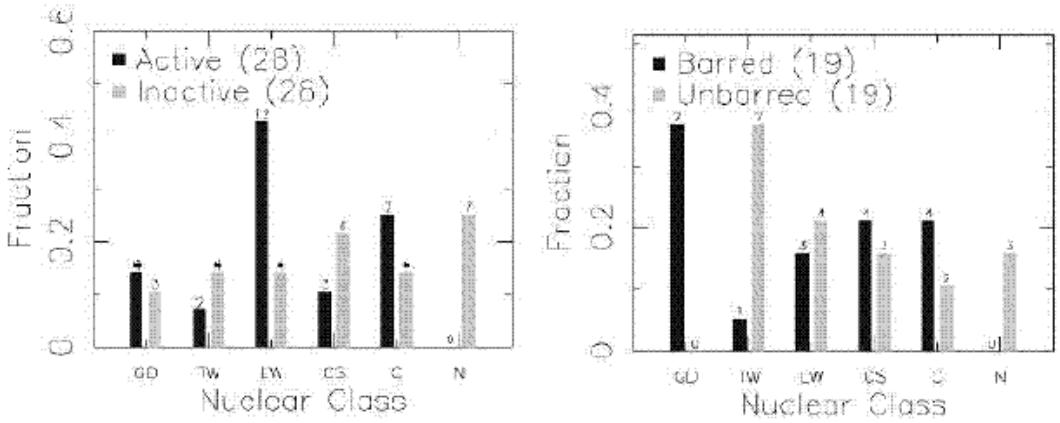

Fig. 12. Nuclear dust spirals in AGN hosts and barred galaxies – *Left:* Distribution of matched samples of 28 active and 28 inactive galaxies. The nuclear dust morphology is divided into six classes denoted as GD: grand-design nuclear dust spiral, TW: tightly wound nuclear spiral, LW: loosely wound nuclear spiral, CS: chaotic spiral, C: chaotic dust structure, N: no dust structure present. The total number of galaxies in each class is shown in parentheses and is used to normalize the histogram bars. Nuclear spirals occur with comparable frequency in active and inactive nuclei. *Right:* Same as above, but for the matched sample of 19 barred and 19 unbarred galaxies. Grand-design nuclear spirals are found only in barred galaxies. (Adapted from Martini et al. 2003)

low level AGN activity. The study also reports that grand-design nuclear dust spirals are found only in galaxies with a large-scale bar, consistent with afore-mentioned idea that these features form via bar-driven gaseous SDWs (Fig. 11).

9 From Hundred pc to Sub-pc Scales

It is far from understood how gas is driven from scales of 100 pc down to sub-pc scales where few direct observational constraints exist. At 100 pc, matter still needs to reduce *its specific angular momentum L by a factor of more than 100* before it can reach sub-pc scales, and eventually the last stable radius of a massive BH (see Fig. 2). I discuss a few mechanisms without attempting to do an exhaustive review:

- *Dynamical friction and feedback from SF:* We already discussed dynamical friction in the context of minor mergers where satellite galaxies located at tens of kpc sink towards the disk of the parent galaxy (§ 5.2) while inducing non-axisymmetric instabilities in this disk. Since dynamical friction

operates on a timescale which is $\propto (R^2\ v/M\ \ln\Lambda)$, it becomes increasingly important for massive gas clumps located at small radii. For instance, Jogee et al. (1999) estimate that $t_{df} \sim 5 \times 10^7$ for a $M \sim 10^8$ $M_\odot$ gas clump at $R \sim 700$ pc using the approximation below:

$$t_{\rm df} = 7 \times 10^7 \text{ yr } \left(\frac{M}{10^8 M_\odot}\right)^{-1} \left(\frac{V_{\rm c}}{300\ km\ s^{-1}}\right) \left(\frac{R}{700 \text{ pc}}\right)^2 \quad (6)$$

Feedback effects from powerful circumnuclear starbursts of several $M_\odot$ yr^{-1} which are common in the central few hundred pc of galaxies (e.g., Jogee et al. 2004c) may also contribute towards removing angular momentum in localized clouds.

- *Tidal Disruption of Gas Clumps:* Numerical investigations by Bekki (2000) suggest that once clumps get down to tens of pc (for instance via dynamical friction), the tidal gravitational field of the MBH transforms the clump into a moderately thick gaseous disk or torus. A few percent of the gas mass (corresponding to a few $\times 10^5$ $M_\odot$) can be subsequently transferred from this gaseous disk to the central sub-parsec region around the MBH within a few $\times 10^6$ yr via viscous torques.
- *Runaway self-gravitational instabilities:* It has been suggested that in a gas-rich nuclear disk, self-gravitational instabilities on repeatedly small scales could lead to three or more bars which are nested within each other (e.g., Shlosman et al. 1990). However, while the presence of three nested bars or triaxial features have been reported in a handful of active galaxies (e.g., Friedli et al. 1996; Laine et al. 2002), the current limited spatial resolution of NIR surveys and molecular gas surveys does not yet allow systematic observational tests of this scenario.
- *Stellar mass loss and disruption of stellar clusters:* As pointed out by Ho et al. (1997b), nominal stellar mass loss rates of $\sim 10^{-5}$–10^{-6} $M_\odot$ yr^{-1} in the central regions of galaxies with luminosity densities of 10^3–10^4 $M_\odot$ pc^{-3} may provide enough fuel for low luminosity AGN. However, while the mass loss rates may be adequate, we yet have to identify mechanisms which can reduce the specific angular momentum of the gas down to 10^{24} cm^2 s^{-1} (see Fig. 2). In the same vein, the tidal disruption of stellar clusters (Emsellem & Combes 1997; Bekki 2000) passing by a central MBH in the accretion disk has been invoked as a source of fuel. However, it still remains to be investigated how exactly the angular momentum of such clusters would be drained and whether this is facilitated by clusters on radial orbits.
- *On pc scales:* On pc ands sub-pc scales viscous torques (e.g., Shlosman et al. 1989; Pringle 1996), warping induced in an accretion disk due to radiation pressure from a central source (Pringle 1996), and hydromagnetic outflows in AGN (Emmering, Blandford, & Shlosman 1992) have been invoked. In the latter model, it is postulated that a hydromagnetic wind containing dense molecular clouds is accelerated radiatively and centrifu-

gally away from an accretion disk, removing angular momentum from the disk, and forming the broad emission lines seen in AGN (Emmering et al. 1992).

10 Summary and Future Perspectives

Faced with the fallible task of providing an 'objective' summary of this review, I can only forewarn the reader with these perennial words:

> *To command the professors of astronomy to confute their own observations is to enjoin an impossibility, for it is to command them to not see what they do see, and not to understand what they do understand, and to find what they do not discover. - Galileo Galilei*

1. **Symbiotic evolution of BHs and bulges:** The mass of a central BH appears to be tightly correlated with the stellar velocity dispersion of the bulge of the host galaxy. SMBHs with a wide range of masses (10^6–10^{10} $M_\odot$) follow the same $M_{\rm bh}$–σ relation, although they reside in a wide array of host galaxies including quiescent early-type (E/S0 Sb–Sc) galaxies, local Seyferts, and luminous QSOs out to $z \sim 3$. Numerous variants of the $M_{\rm bh}$–σ relation have by now been proposed, including tight correlations between $M_{\rm bh}$ and quantities such as the bulge luminosity, the light concentration of galaxies, the Sersic index, and the mass of the DM halo. It thus appears that active and quiescent BHs bear a common relationship to the surrounding triaxial component of their host galaxies over a wide range of cosmic epochs and BH masses. This points towards a symbiotic evolution of BHs and the central triaxial features of their hosts.
2. **Census and growth epoch of BHs:** A census of the BH mass density at different epochs suggests that accretion with a standard radiative efficiency during the quasar era (z=0.2–5) can readily account for the BH mass density (few $\times$ 10^5 $M_\odot$ Mpc^{-3}) found in local ($z < 0.1$) early-type galaxies. Furthermore, only a small fraction of this local BH mass density is in the form of active Seyfert galaxies, and in the latter systems, the inferred mass accretion rates at the BH are typically 10^3 times lower than in QSOs. Taken together, the evidence suggests that there is no significant growth of BHs at the present epoch compared to the quasar era. Therefore, in the context of AGN fueling, we should bear in mind that the dominant fueling mechanisms for luminous QSOs out to $z \sim 2.5$ may be markedly different from those impacting local Seyferts. For instance, tidal interactions and mergers are likely to be more important in activating AGN activity at early epochs than in the present-day.
3. **The angular momentum problem:** One of the most important challenges in fueling AGN is arguably the angular momentum problem. The

specific angular momentum (L) of matter located at a radius of a few kpc must be reduced by more than 10^5 before it is fit for consumption by a BH (Fig. 2). The angular momentum barrier is a more daunting challenge than the amount of gas *per se* . For instance, while there may be ample material (e.g., 10^6 $M_\odot$ clouds) in the inner 200 pc radius to fuel typical Seyferts over nominal duty cycles (10^8 years), the challenge is to understand what fueling mechanisms can drain their angular momentum by 99.99% so that they are digestible by a BH.

4. **Fueling mechanisms on different scales:** There is no universal fueling mechanism which operates efficiently on all spatial scales, from several kpc all the way down to the last stable orbit of a BH. Instead, different fueling mechanisms such as gravitational torques (e.g., from large-scale bars and nuclear bars), dynamical friction (on massive circumnuclear gas clumps), hydrodynamical torques (shocks), and viscous torques may relay each other at different radii in terms of their effectiveness in draining angular momentum. According to simulations, large-scale bars (whether spontaneously or tidally induced) are the most efficient mechanisms for driving large gas inflows from several kpc down to the inner few hundred pc. This holds not only in the case of an isolated barred galaxy, but also for some classes of minor (1:10) mergers, most intermediate (1:3) mass ratio mergers, and the early phases of most major (1:1) mergers. During the late stages of a major merger, strongly-varying gravitational torques and strong shocks on crossing orbits can subsequently drive the circumnuclear gas further in at large rates ($\gg 1$ $M_\odot$ yr^{-1}).
5. **Correlations between AGN and interactions:** Statistically significant correlations between morphological signs of interactions and AGN are seen in systems with high mass accretion rates ($\dot{M} \geq 10$ $M_\odot$ yr^{-1}) such as very luminous or radio-loud QSOs. The presence of a correlation only at very high mass accretion rates holds to reason because such accretion rates are primarily realized in nature during violent processes such as major/intermediate mass-ratio interactions. However, it must be noted that the reverse does not hold true: not *all* major interactions lead to extreme activity because their effectiveness in inducing large gas inflows depend on many merger parameters (speeds, energies, spin-orbital angular momenta alignments).
   For moderate luminosity QSOs and typical Seyferts, no clear correlation between activity and interactions is seen. The lack of a correlation may be due to the fact that the low $\dot{M}$ required in Seyferts and lower luminosity QSOs can be provided not only by strong fueling mechanisms such as interactions which impact the bulk of the gas, but also by localized low-energetic processes which impact only 10^{-3}–10^{-2} of the circumnuclear gas (see § 5.4).
6. **Correlations between AGN and host galaxy properties:**

- Local AGN (Sy 1 and Sy 2) and moderate luminosity ($M_{\rm B} \simeq$ -23) AGN in the redshift range z=0.4–1.1 tend to reside primarily in early-type (bulge-dominated) galaxies.
- AGN early-type hosts show enhanced blue global rest-frame optical colors compared to early-type inactive galaxies. This holds in low redshift ($z < 0.2$) SDSS studies, as well as in intermediate redshifts ($z \sim 0.5$–1.1) samples. These colors are consistent with the presence of young stellar populations, suggesting that the onset of AGN activity is intimately linked to the recent onset of global SF in the hosts.
- The frequency of large-scale stellar bars is significant higher in starburst galaxies than normal galaxies. The bar–starburst correlation is consistent with the idea that a bar efficiently drains angular momentum of gas on exactly the right spatial scales (several kpc to a few hundred pc; Fig 2) relevant for building the pre-requisite large gas concentrations for circumnuclear starbursts. At this time, the question of whether Seyferts have an excess of large-scale bars compared to inactive galaxies remains open. Studies based on high resolution NIR images, different samples, and different bar identification methods (ellipse fits, Fourier methods) yield different conflicting results. The reader is referred to § 6.3 for a detailed discussion.
- Seyferts appear to have *weaker* bar strengths compared to inactive galaxies. These results may lend observational support to the long-claimed (but little-tested) idea that a large build-up of mass concentration via gas inflow into the inner 100 pc can weaken or even destroy the large-scale bar. However, the question of whether bars are long-lived or whether they dissolve and reform recurrently over a Hubble time is also highly controversial at the moment (§ 6.1).
- The frequency of outer rings and of (inner + outer) rings appears to be higher by a factor of 3-4 in Seyfert galaxies compared to normal galaxies. Various interpretations of this strong correlation have been proposed. The rings may be weak non-axisymmetric oval distortions or they be remnants of dissolved bars. Alternatively, the correlation may be the result of both Seyferts and rings existing preferentially in early-type systems.
- The frequency of both nuclear stellar bars (identified morphologically) and nuclear dust spirals is found to be similar in Seyferts and normal galaxies. This lack of correlation suggests that these features are not universal mechanisms for fueling an AGN or/and that their lifetime is short ($\leq$ few $\times 10^8$ years).

7. **Future perspectives:** I outline below a few of the many exciting developments in AGN research we might wish/expect in the upcoming decade. *(a)* Now that we have a relatively solid census of BH mass density from $z \sim$ 0.1–5 (§ 4), we need to systematically map the molecular gas content and structural properties of AGN hosts as a function of redshift in

order to investigate why AGN activity has declined sharply since $z \sim$2.5. NIR integral field spectroscopy on 8m-class telescopes, inflowing 24 μm *Spitzer* data, and the advent of sub-millimeter facilities like the 50-m LMT (*circa* 2007) and ALMA (*circa* 2010) will provide key constraints. *(b)* To date, all studies between AGN/starbursts and large-scale bars have focused on local galaxies. Yet, both the cosmic SFR density and AGN activity increase out to t $z \sim 1$. The ongoing work on the impact of bars and interactions over the last 9 Gyr (out to $z \sim 1.3$) on central starbursts and AGN based on the GEMS *HST* survey and Chandra Deep Field South data (Jogee et al. 2004a,b) will help constrain how bars and external triggers relate to the activities and structural evolution of galaxies at these epochs. *(c)* There is a dire lack of high resolution interferometric observations of molecular gas for a *statistically significant sample* of AGN, even locally Three ongoing surveys are alleviating this problem. The Molecular gas in Active and Inactive Nuclei (MAIN; Jogee, Baker, Sakamoto, & Scoville 2001) high resolution, multi-line survey covers forty (Seyfert, LINER, and HII) nuclei. MAIN aims at constraining the drivers of activity levels in galactic nuclei, and complements the ongoing Nuclei of GAlaxies (NUGA) survey (Garcia-Burillo et al. 2003) and the multiple line survey of Seyferts (Kohno et al. 2001); *d)* The advent of large (30–100 m) diffraction-limited telescopes such as the Giant Magellan Telescope will help test/extend the $M_{\rm bh}$–σ relation for late-type spirals, IMBHs, and low surface brightness ellipticals.

11 Acknowledgements

For comments and discussions, I thank numerous colleagues, in particular, L. Ferrarese, R. van der Marel, F. Combes, S. Laine, the GEMS collaboration, I. Shlosman, N. Grogin, J. H. Knapen, & L. Hernquist. I acknowledge support from the National Aeronautics and Space Administration (NASA) under LTSA Grant NAG5-13063 issued through the Office of Space Science.

References

1. Adams, F. C., Graff, D. S., & Richstone, D. O. 2001, ApJL, 551, L31
2. Athanassoula, E. 1992, MNRAS, 259, 328
3. Bahcall, J. N., Kirhakos, S., Saxe, D. H., & Schneider, D. P. 1997, ApJ, 479, 642
4. Baker, A. J. 2000, Ph.D. thesis, California Institute of Technology
5. Balick, B. & Heckman, T. M. 1982, ARAA, 20, 431
6. Barnes, J. E. & Hernquist, L. E. 1991, ApJL, 370, L65
7. Barnes, J. E. & Hernquist, L. 1996, ApJ, 471, 115
8. Bekki, K. 2000, ApJ, 545, 753

9. Baumgardt, H., Makino, J., Hut, P., McMillan, S., & Portegies Zwart, S. 2003, ApJL, 589, L25
10. Benedict, G. F., Smith, B. J., & Kenney, J. D. P. 1996, AJ, 112, 1318
11. Binney, J. & Tremaine, S. 1987, Princeton, NJ, Princeton University Press, 1987
12. Blandford, R. D. & McKee, C. F. 1982, ApJ, 255, 419
13. Blandford, R. D. & Begelman, M. C. 1999, MNRAS, 303, L1
14. Böker, T., van der Marel, R. P., & Vacca, W. D. 1999, AJ, 118, 831
15. Bournaud, F. & Combes, F. 2002, A&A, 392, 83
16. Bromm, V. & Loeb, A. 2003, ApJ, 596, 34
17. Burkert, A. & Silk, J. 2001, ApJL, 554, L151
18. Buta, R. & Combes, F. 1996, Fundamentals of Cosmic Physics, 17, 95
19. Carollo, C. M., Stiavelli, M., & Mack, J. 1998, AJ, 116, 68
20. Cid Fernandes, R., Heckman, T., Schmitt, H., Delgado, R. M. G., & Storchi-Bergmann, T. 2001, ApJ, 558, 81
21. Chokshi, A. & Turner, E. L. 1992, MNRAS, 259, 421
22. Colbert, E. J. M., & Miller, M. C. 2005 (astro-ph/0402677)
23. Combes, F. & Gerin, M. 1985, A&A, 150, 327 Combes 1994;
24. Combes, F. 2003, ASP Conf. Ser. 290: Active Galactic Nuclei: From Central Engine to Host Galaxy, eds. S. Collin, F. Combes, & I. Shlosman (ASP), 411
25. Contopoulos, G. & Papayannopoulos, T. 1980, A&A, 92, 33
26. Cowie, L. L., & Barger, A. J., Chapter 9, "Supermassive Black Holes in the Distant Universe", ed. A. J. Barger, Kluwer Academic Publishers, in press
27. Di Matteo, T., Croft, R. A. C., Springel, V., & Hernquist, L. 2003, ApJ, 593, 56
28. Filippenko, A. V. & Ho, L. C. 2003, ApJL, 588, L13
29. de Vaucouleurs, G., de Vaucouleurs, A., Corwin, H. G., Buta, R. J., Paturel, G., & Fouque, P. 1991, Volume 1-3, XII, Springer-Verlag
30. Dahari, O. 1984, AJ, 89, 966
31. Disney, M. J., et al. 1995, Nature, 376, 150
32. Dubinski, J. 1994, ApJ, 431, 61
33. Ebisuzaki, T., et al. 2001, ApJL, 562, L19
34. El-Zant, A. A., Shlosman, I., Begelman, M. C., & Frank, J. 2003, ApJ, 590, 641
35. Elmegreen, B. G. 1994, ApJ, 427, 384
36. Elmegreen, B. G., et al. 1998, ApJL, 503, L119
37. Elmegreen, D. M., Elmegreen, B. G., & Eberwein, K. S. 2002, ApJ, 564, 234
38. Emmering, R. T., Blandford, R. D., & Shlosman, I. 1992, ApJ, 385, 460
39. Englmaier, P. & Shlosman, I. 2000, ApJ, 528, 677
40. Erwin, P. & Sparke, L. S. 2002, AJ, 124, 65
41. Erwin, P. 2004, A&A, 415, 941
42. Eskridge, P. B., et al. 2002, ApJS, 143, 73
43. Fabian, A. C. & Iwasawa, K. 1999, MNRAS, 303, L34
44. Ferrarese, L. 2002, ApJ, 578, 90
45. Ferrarese, L. 2002, Current high-energy emission around black holes, 3
46. Ferrarese, L., Pogge, R. W., Peterson, B. M., Merritt, D., Wandel, A., & Joseph, C. L. 2001, ApJL, 555, L79
47. Ferrarese, L. & Merritt, D. 2000, ApJL, 539, L9
48. Ferrarese, L. & Ford, H. C. 1999, ApJ, 515, 583

49. Ferrarese, L., Ford, H. C., & Jaffe, W. 1996, ApJ, 470, 444
50. Friedli, D. & Martinet, L. 1993, A&A, 277, 27
51. Friedli, D. & Benz, W. 1993, A&A, 268, 65
52. Friedli, D., Wozniak, H., Rieke, M., Martinet, L., & Bratschi, P. 1996, A&A Suppl., 118, 461
53. García-Burillo, S., et al. 2003, A&A, 407, 485
54. Gebhardt, K., et al. 2000, ApJL, 539, L13
55. Gebhardt, K., Rich, R. M., & Ho, L. C. 2002, ApJL, 578, L41
56. Geha, M., Guhathakurta, P., & van der Marel, R. P. 2002, AJ, 124, 3073
57. Genzel, R., Pichon, C., Eckart, A. et al. 2000, MNRAS, 317, 348
58. Gerssen, J., van der Marel, R. P., Gebhardt, K., Guhathakurta, P., Peterson, R. C., & Pryor, C. 2003, AJ, 125, 376
59. Ghez, A. M., et al. 2003, ApJL, 586, L127
60. Giavalisco, M., et al. 2004, ApJL, 600, L93
61. Graham, A. W., Erwin, P., Caon, N., & Trujillo, I. 2001, ApJL, 563, L11
62. Grogin, N. et al. 2004, ApJ, submitted
63. Haehnelt, M. G. & Kauffmann, G. 2000, MNRAS, 318, L35
64. Häring, N. & Rix, H. 2004, ApJL, 604, L89
65. Harms, R. J., et al. 1994, ApJL, 435, L35
66. Hasan, H. & Norman, C. 1990, ApJ, 361, 69
67. Hawarden, T. G., et al. 1986, MNRAS, 221, 41
68. Heckman, T. M., Armus, L., & Miley, G. K. 1990, ApJS, 74, 833
69. Heller, C. H. & Shlosman, I. 1994, ApJ, 424, 84
70. Heller, C., Shlosman, I., & Englmaier, P. 2001, ApJ, 553, 661
71. Hernquist, L. 1989, Nature, 340, 687
72. Hernquist, L. & Mihos, J. C. 1995, ApJ, 448, 41
73. Ho, L. C., Filippenko, A. V., & Sargent, W. L. W. 1997a, ApJS, 112, 315
74. Ho, L. C., Filippenko, A. V., & Sargent, W. L. W. 1997b, ApJ, 487, 591
75. Hummel, E., van der Hulst, J. M., Kennicutt, R. C., & Keel, W. C. 1990, A&A, 236, 333
76. Hunt, L. K. & Malkan, M. A. 1999, ApJ, 516, 660
77. Hutchings, J. B., Frenette, D., Hanisch, R., Mo, J., Dumont, P. J., Redding, D. C., & Neff, S. G. 2002, AJ, 123, 2936
78. Hutchings, J. B. 1987, ApJ, 320, 122
79. Jahnke, K. et al. 2004, ApJ, in press
80. Jogee, S., Kenney, J. D. P., & Smith, B. J. 1998, ApJL, 494, L185
81. Jogee, S., Kenney, J. D. P., & Smith, B. J. 1999, ApJ, 526, 665
82. Jogee, S. 1999, Ph.D. Thesis, Yale University
83. Jogee, S., Baker, A. J., Sakamoto, K., Scoville, N. Z., & Kenney, J. D. P. 2001, ASP Conf. Ser. 249: The Central Kiloparsec of Starbursts and AGN: The La Palma Connection, 612
84. Jogee, S., Knapen, J. H., Laine, S., Shlosman, I., Scoville, N. Z., & Englmaier, P. 2002a, ApJL, 570, L55
85. Jogee, S., Shlosman, I., Laine, S., Englmaier, P., Knapen, J. H., Scoville, N. Z., & Wilson, C. D. 2002b, ApJ, 575, 156
86. Jogee, S., et al. 2003, IAU Symposium, 216
87. Jogee, S., Rix, H.-W., Barazza, F., Heyer, I., Davies, J., Shlosman, I., Lubell, G., et al. 2004a, in Penetrating Bars through Masks of Cosmic Dust eds. D. Block, K. Freeman, R. Groess, I. Puerari, & E.K. Block (Dordrecht: Kluwer), in press.

88. Jogee, S., Rix, H.-W., Barazza, F., Heyer, I., Davies, J., Shlosman, I., Lubell, G., et al. 2004b, ApJL, submitted
89. Jogee, S., Scoville, N. Z., & Kenney, J. 2004c, ApJ, in press
90. Kaspi, S., Smith, P. S., Netzer, H., Maoz, D., Jannuzi, B. T., & Giveon, U. 2000, ApJ, 533, 631
91. Kauffmann, G., et al. 2003, MNRAS, 346, 1055
Keel, W. C., Kennicutt, R. C., Hummel, E., & van der Hulst, J. M. 1985, AJ, 90, 708
92. Kenney, J. D. P., Wilson, C. D., Scoville, N. Z., Devereux, N. A., & Young, J. S. 1992, ApJL, 395, L79
93. Kennicutt, R. C., Roettiger, K. A., Keel, W. C., van der Hulst, J. M., & Hummel, E. 1987, AJ, 93, 1011
94. Kirhakos, S., Bahcall, J. N., Schneider, D. P., & Kristian, J. 1999, ApJ, 520, 67
95. Knapen, J. H., Beckman, J. E., Heller, C. H., Shlosman, I., & de Jong, R. S. 1995, ApJ, 454, 623
96. Knapen, J. H., Shlosman, I., & Peletier, R. F. 2000, ApJ, 529, 93
97. Knapen, J. H. 2004, ASP Conf. Ser.: The Neutral ISM in Starburst Galaxies, eds. S. Aalto, S. Hüttemeister, & A. Pedlar, in press (astro-ph/0312172)
98. Kohno, K., et al. 2001, ASP Conf. Ser. 249: The Central Kiloparsec of Starbursts and AGN: The La Palma Connection, 672
99. Kormendy, J. & Richstone, D. 1995, ARAA, 33, 581
100. Laine, S., Shlosman, I., & Heller, C. H. 1998, MNRAS, 297, 1052
101. Laine, S., Knapen, J. H., Perez-Ramirez, D., Doyon, R., & Nadeau, D. 1999, MNRAS, 302, L33
102. Laine, S., Shlosman, I., Knapen, J. H., & Peletier, R. F. 2002, ApJ, 567, 97
103. Laurikainen, E. & Salo, H. 1995, A&A, 293, 683
104. Laurikainen, E., Salo, H., & Rautiainen, P. 2002, MNRAS, 331, 880
105. Laurikainen, E., Salo, H., & Buta, R. 2004, ApJ, 607, 103
106. Lehnert, M. D., Heckman, T. M., Chambers, K. C., & Miley, G. K. 1992, ApJ, 393, 68
107. Lynden-Bell, D. 1969, Nature, 223, 690
108. Maciejewski, W. & Sparke, L. S. 2000, MNRAS, 313, 745
109. Maciejewski, W., Teuben, P. J., Sparke, L. S., & Stone, J. M. 2002, MNRAS, 329, 502
110. Martin, P. & Roy, J. 1994, ApJ, 424, 599
111. Martini, P. & Pogge, R. W. 1999, AJ, 118, 2646
112. Martini, P., Regan, M. W., Mulchaey, J. S., & Pogge, R. W. 2003, ApJ, 589, 774
113. Martini, P. 2004, in Proc. IAU 222: The Interplay among Black Holes, Stars and ISM in Galactic Nuclei, eds. Th. Storchi Bergmann, L. C. Ho, & H. R. Schmitt, in press
114. Merritt, D. & Ferrarese, L. 2001, MNRAS, 320, L30
115. Mihos, J. C. & Hernquist, L. 1996, ApJ, 464, 641
116. Mihos, J. C., Walker, I. R., Hernquist, L., Mendes de Oliveira, C., & Bolte, M. 1995, ApJL, 447, L87
117. Miyoshi, M., et al. 1995, Nature, 373, 127
118. Mobasher, B., Jogee, S., Dahlen, T., de Mello, D., Lucas, R. A., Conselice, C. J., Grogin, N. A., & Livio, M. 2004, ApJL, 600, L143

119. Mulchaey, J. S. & Regan, M. W. 1997, ApJL, 482, L135
120. Naab, T. & Burkert, A. 2001, ASP Conf. Ser. 230: Galaxy Disks and Disk Galaxies, 451
121. Narayan, R., Igumenshchev, I. V., & Abramowicz, M. A. 2000, ApJ, 539, 798
122. Negroponte, J. & White, S. D. M. 1983, MNRAS, 205, 1009
123. Noguchi, M. 1988, A&A, 203, 259
124. Norman, C. & Scoville, N. 1988, ApJ, 332, 124
125. Norman, C. A., Sellwood, J. A., & Hasan, H. 1996, ApJ, 462, 114
126. Ostriker, J. P. & Tremaine, S. D. 1975, ApJL, 202, L113
127. Padovani, P., Burg, R., & Edelson, R. A. 1990, ApJ, 353, 438
128. Petitpas, G. R. & Wilson, C. D. 2003, ApJ, 587, 649
129. Peterson, B. M. 1993, PASP, 105, 247
130. Pringle, J. E. 1996, MNRAS, 281, 357
131. Quillen, A. C., Frogel, J. A., Kenney, J. D. P., Pogge, R. W., & Depoy, D. L. 1995, ApJ, 441, 549
132. Quinn, P. J., Hernquist, L., & Fullagar, D. P. 1993, ApJ, 403, 74
133. Regan, M. W., Vogel, S. N., & Teuben, P. J. 1997, ApJL, 482, L143
134. Regan, M. W. & Mulchaey, J. S. 1999, AJ, 117, 2676
135. Richstone, D., et al. 1998, Nature, 395, A14
136. Rix, H., et al. 2004, ApJS, 152, 163
137. Rees, M. J. 1984, ARAA, 22, 471
138. Roberts, M. S. & Haynes, M. P. 1994, ARAA, 32, 115
139. Sakamoto, K., Okumura, S. K., Ishizuki, S., & Scoville, N. Z. 1999, ApJ, 525, 691
140. Sanchez, S. et al. 2004,ApJ, in press
141. Sanders, D. B. & Mirabel, I. F. 1996, ARAA, 34, 749
142. Schmitt, H. R. 2001, AJ, 122, 2243
143. Schwarz, M. P. 1984, MNRAS, 209, 93
144. Shen, J. & Sellwood, J. A. 2004, ApJ, 604, 614
145. Sheth, K., Regan, M. W., Scoville, N. Z., & Strubbe, L. E. 2003, ApJL, 592, L13
146. Shields, G. A., Gebhardt, K., Salviander, S., Wills, B. J., Xie, B., Brotherton, M. S., Yuan, J., & Dietrich, M. 2003, ApJ, 583, 124
147. Shimada, M., Ohyama, Y., Nishiura, S., Murayama, T., & Taniguchi, Y. 2000, AJ, 119, 2664
148. Shlosman, I., Frank, J., & Begelman, M. C. 1989, Nature, 338, 45
149. Shlosman, I. & Begelman, M. C. 1989, ApJ, 341, 685
150. Shlosman, I., Begelman, M. C., & Frank, J. 1990, Nature, 345, 679
151. Shlosman, I., Peletier, R. F., & Knapen, J. H. 2000, ApJL, 535, L83
152. Shlosman, I. & Heller, C. H. 2002, ApJ, 565, 921
153. Shlosman, I. 2003, ASP Conf. Ser. 290: Active Galactic Nuclei: From Central Engine to Host Galaxy, , eds. S. Collin, F. Combes, & I. Shlosman (Astronomical Society of the Pacific), 427
154. Schödel, R., Ott, T., Genzel, R., Eckart, A., Mouawad, N., & Alexander, T. 2003, ApJ, 596, 1015
155. Soltan, A. 1982, MNRAS, 200, 11
156. Storchi-Bergmann, T., et al. 2001, ApJ, 559, 147
157. Struck, C. 1997, ApJS, 113, 269
Terlevich, R., Melnick, J., & Moles, M. 1987, IAU Symp. 121: Observational Evidence of Activity in Galaxies, 121, 499

158. Tremaine, S., et al. 2002, ApJ, 574, 740
159. Veilleux, S., Kim, D.-C., & Sanders, D. B. 2001, QSO Hosts and Their Environments, 165
160. van der Marel, R. P. & van den Bosch, F. C. 1998, AJ, 116, 2220
161. van der Marel, R. P. 2003, in Carnegie Observatories Astrophysics Series, Vol. 1, Coevolution of Black Holes and Galaxies, ed. L. C. Ho (Cambridge University Press)
162. Wada, K. & Norman, C. A. 2001, ApJ, 547, 172
163. Walker, I. R., Mihos, J. C., & Hernquist, L. 1996, ApJ, 460, 121
164. Wandel, A., Peterson, B. M., & Malkan, M. A. 1999, ApJ, 526, 579
165. Wozniak, H., Friedli, D., Martinet, L., Martin, P., & Bratschi, P. 1995, A&A Suppl., 111, 115
166. Wyithe, J. S. B. & Loeb, A. 2003, ApJ, 595, 614
167. Yates, M. G., Miller, L., & Peacock, J. A. 1989, MNRAS, 240, 129
168. Yu, Q. & Tremaine, S. 2002, MNRAS, 335, 965